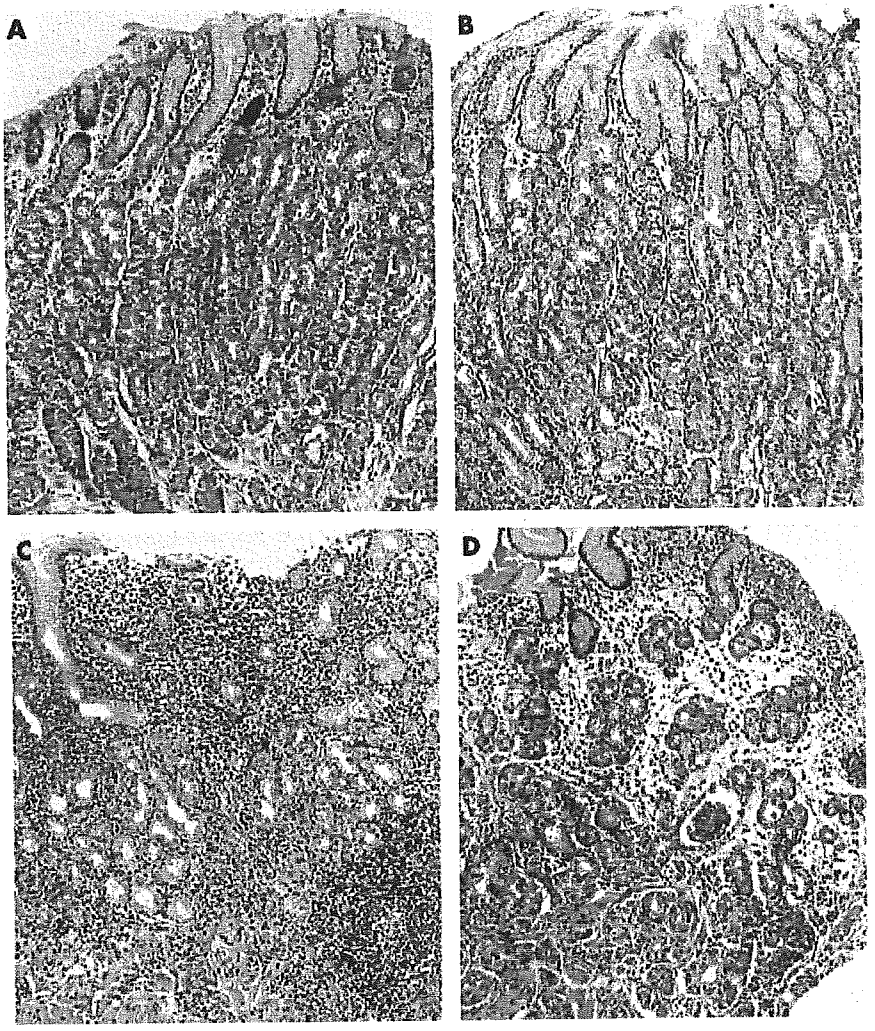

Figure 5 Representative images of biopsy specimens stained with haematoxylin-eosin used for histological assessment of gastric atrophy. The fundic mucosa before (A) and after (B) eradication in the non-severe atrophic group is shown for a subject with a pepsinogen I/II ratio of 4.7 before treatment. The fundic mucosa before (C) and after (D) eradication in the severe atrophic group is shown for a subject with a pepsinogen I/II ratio of 1.0 before treatment. The pepsinogen I/II ratio was closely correlated with gastric body atrophy grade assessed by histological examination.

shown in fig 2B and 2C, the increase in mRNA expression levels of anion exchanger 2 (n = 111) and M3 muscarinic receptor (n = 111) after *H pylori* eradication was 2.3- and 2.5-fold, respectively, similar to intrinsic factor (n = 111) (fig 4). These data indicate that *H pylori* eradication predominantly restored H^+/K^+-ATPase expression compared with other molecules expressed in parietal cells. As *H pylori* eradication did not alter parietal cell numbers in the gastric mucosa, these data suggest that recovery of gastric acid secretion after *H pylori* eradication in the gastric mucosa is due to an increase in H^+/K^+-ATPase expression in parietal cells.

Grade of gastric atrophy did not affect restoration levels of H^+/K^+-ATPase mRNA expression after *H pylori* eradication

Based on the finding that *H pylori* eradication restores H^+/K^+-ATPase expression in parietal cells, we then examined whether restoration of H^+/K^+-ATPase expression in parietal cells was related to the degree of gastric atrophy before *H pylori* eradication. We thus compared gastric H^+/K^+-ATPase mRNA expression levels between the groups with different degrees of gastric atrophy. Pepsinogen I and pepsinogen II differ in their location in the stomach. Both are located in chief and mucous neck cells of the oxyntic gland mucosa in the gastric corpus but only pepsinogen II is present in the gastric antrum. A pepsinogen I/II ratio <3 is considered to be a reliable marker for severe atrophic gastritis.[11 12] We thus evaluated gastric atrophy in subjects by determining the pepsinogen I/II ratio. In addition, gastric atrophy was evaluated by histological examination. Figure 5 shows representative images of biopsy specimens stained with haematoxylin-eosin used for histological assessment of gastric atrophy. In these cases, the pepsinogen I/II ratio was closely correlated with the gastric atrophy grade assessed by histological examination. We thus classified subjects into two groups using the pepsinogen I/II ratio as a gastric atrophy parameter: severe atrophy group (n = 66) (pepsinogen I/II ratio <3) and non-severe atrophy group (n = 45) (pepsinogen I/II ratio ≥3). As shown in fig 6, median H^+/K^+-ATPase mRNA expression levels were increased from 0.9 to 960 in the severe atrophy group, and from 37 to 1273 in the non-severe atrophy group, respectively. These results indicate that H^+/K^+-ATPase expression in parietal cells is largely restored even in patients with high grade gastric atrophy.

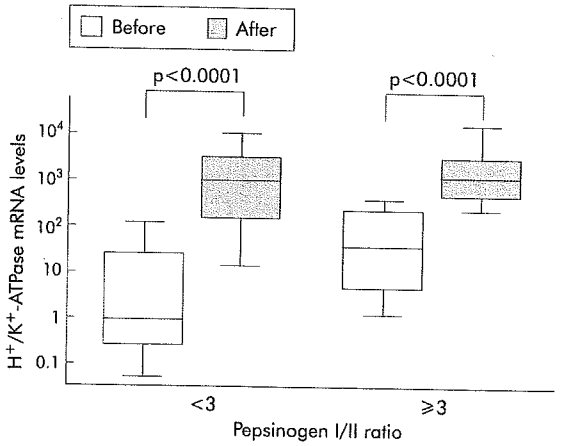

Figure 6 Comparison of H^+/K^+-ATPase mRNA expression levels in the oxyntic mucosa and serum pepsinogen levels before and after *Helicobacter pylori* cure. H^+/K^+-ATPase mRNA expression levels rose markedly despite the serum pepsinogen I/II ratio (0.9 (0.3–24) and 960 (148–3106) (median (1st quartile–3rd quartile)) in the severe atrophy group (pepsinogen I/II ratio<3) ($p<0.0001$); 37 (5.0–219) and 1273 (479–3343) in non-severe atrophy group (pepsinogen I/II ratio ≥3) ($p<0.0001$ by Wilcoxon rank sum test)).

DISCUSSION

In the present study we have demonstrated restoration of H^+/K^+-ATPase mRNA expression levels in the gastric mucosa at a relatively early stage after *H pylori* eradication without alteration of parietal cell numbers. In contrast, restoration of anion exchanger 2, M3 muscarinic receptor, and intrinsic factor mRNA expression levels in the gastric mucosa after *H pylori* eradication was much smaller than that of H^+/K^+-ATPase. These results suggest that restoration of H^+/K^+-ATPase expression in parietal cells plays a central role in the recovery of gastric acid secretion after *H pylori* eradication.

It is well known that gastric acid secretion recovers after *H pylori* eradication but the mechanism has been unclear, partly due to the controversy as to whether *H pylori* eradication leads to improvement of gastric atrophy. Tucci *et al* indicated that there was a significant improvement in mucosal inflammation and atrophy in the corpus one year after eradication.[13] However, several reports showed that gastric atrophy did not improve after eradication.[14–17] Hence it has been unclear whether recovery of gastric acid secretion is a result of restoration of parietal cell numbers or functional recovery of parietal cells. Our current study simultaneously demonstrated absence of alteration of parietal cell number and restoration of H^+/K^+-ATPase, thus providing strong evidence that recovery of gastric acid secretion after *H pylori* eradication is caused by functional recovery of parietal cells.

The mechanism of the inhibitory effect of *H pylori* infection on gastric acid secretion is still controversial, despite extensive studies. One hypothesis is that parietal cell function is directly affected by *H pylori*. It has been shown in vivo that acute infection with *H pylori* causes hypochlorhydria.[18] In an in vitro experiment using human gastric adenocarcinoma (AGS) cells transfected with H^+/K^+-ATPase α 5′-flanking sequence, *H pylori* infection induced dose dependent inhibition of basal and histamine stimulated H^+/K^+-ATPase α promoter activity by 80% and 66%, respectively.[19] Smolka *et al* demonstrated that *H pylori* downregulated human H^+/K^+-ATPase α basal transcription by displacement of the AP-1 transcription factor from the homology box I region of H^+/K^+-ATPase α 5′-flanking sequence.[20] In our study, restoration of gastric H^+/K^+-ATPase after eradication of *H pylori* strongly suggests that inhibition of H^+/K^+-ATPase production in gastric parietal cells during *H pylori* infection plays a role. One possible explanation is the association with inflammatory responses induced by *H pylori* infection. Antibacterial treatment is known to induce resolution of the acute component of *H pylori* gastritis within a few days after treatment.[21] IL-1β is important in initiating and amplifying the inflammatory response against bacteria and is also a potent inhibitor of gastric acid secretion.[22–26] Indeed, our data showed a negative association between H^+/K^+-ATPase and IL-1β, supporting this notion. These results also suggest that *H pylori* derived ammonia may not be responsible for the reversible inhibition of acid secretion, as several investigators have reported.[27 28]

Gastric acid secretion from parietal cells is highly organised, with a stimulus-secretion coupling molecular system. In parietal cells, neurohormonal stimuli trigger parietal acid secretion through receptors present in the basolateral membranes, such as M3 muscarinic receptor.[29–31] Then, H^+/K^+-ATPase is transported to the apical membrane where it secretes acid into the gastric lumen. During acid secretion, anion exchanger 2 plays a role in acid loading into parietal cells by functioning in $HCO3^-$ efflux and Cl^- influx across the basolateral membrane.[32 33] Thus H^+/K^+-ATPase, M3 muscarinic receptor, and anion exchanger 2 play crucial roles in parietal gastric acid secretion. Of these molecules, our study clearly demonstrated the extraordinary restoration of H^+/K^+-ATPase after *H pylori* eradication.

Consistent with our data, Furuta *et al* previously reported that both H^+/K^+-ATPase expression and gastric acid secretion are elevated after *H pylori* eradication.[34] These data suggest a relationship between the increase in H^+/K^+-ATPase expression and recovery of gastric acid secretion. However, their data did not address the question of whether the increase in H^+/K^+-ATPase expression was a result of an increase in parietal cell numbers or enhanced expression of H^+/K^+-ATPase. We thus expanded their study by showing that recovery of gastric acid secretion in the gastric mucosa after eradication was not due to an increase in parietal cell numbers but to enhanced expression of H^+/K^+-ATPase in parietal cells. In addition, we elucidated that H^+/K^+-ATPase expression in the gastric mucosa was restored even in patients with severe gastric atrophy. We further extended knowledge of the importance of restoration of H^+/K^+-ATPase expression in the recovery of acid secretion by comparing it with restoration of other molecules involved in parietal acid secretion. Taken together, it is reasonable to conclude that restoration of H^+/K^+-ATPase expression plays a central role in recovery of gastric acid secretion after *H pylori* eradication.

Furuta and colleagues[34] and our group observed restoration of H^+/K^+-ATPase expression at a relatively early period: one month and three months after *H pylori* eradication, respectively. However, recovery of gastric acid secretion has also been observed at later periods after *H pylori* eradication. For example, Iijima *et al* reported that gastrin stimulated acid secretion was observed even seven months after *H pylori* eradication in patients with gastric ulcer.[35] However, changes in parietal cell numbers and H^+/K^+-ATPase expression during these later periods after *H pylori* eradication have yet to be elucidated. Thus further study on parietal cell numbers and H^+/K^+-ATPase expression at late periods after *H pylori* eradication is warranted.

In conclusion, we have shown marked restoration of H^+/K^+-ATPase expression in the gastric mucosa after *H pylori* eradication without alteration of parietal cell numbers. These data provide novel insight into our understanding of the mechanism of gastric functional recovery after treatment of *H pylori* infection.

ACKNOWLEDGEMENTS

We are indebted to Ms Kaoru Tokuda for her excellent technical assistance.

Authors' affiliations

H Osawa, H Kita, H Ohnishi, H Hoshino, H Mutoh, Y Ishino, E Watanabe, K Satoh, K Sugano, Department of Internal Medicine, Division of Gastroenterology, Jichi Medical School, Kawachi, Tochigi, Japan

Conflict of interest: None declared.

REFERENCES

1 **Marshall BJ**, Goodwin CS, Warren JR, *et al.* Prospective double-blind trial of duodenal ulcer relapse after eradication of Campylobacter pylori. *Lancet* 1988;**2**:1437–42.
2 **Labenz J**, Borsch G. Evidence for the essential role of Helicobacter pylori in gastric ulcer disease. *Gut* 1994;**35**:19–22.
3 **Rohrer GV**, Welsh JD. Correlative study: gastric secretion and histology. *Gastroenterology* 1967;**52**:185–91.
4 **Ruiz B**, Correa P, Fontham ET, *et al.* Antral atrophy, Helicobacter pylori colonization, and gastric pH. *Am J Clin Pathol* 1996;**105**:96–101.
5 **Gutierrez O**, Melo M, Segura AM, *et al.* Cure of Helicobacter pylori infection improves gastric acid secretion in patients with corpus gastritis. *Scand J Gastroenterol* 1997;**32**:664–8.
6 **El-Omar EM**, Oien K, El-Nujumi A, *et al.* Helicobacter pylori infection and chronic gastric acid hyposecretion. *Gastroenterology* 1997;**113**:15–24.
7 **Bercik P**, Verdu EF, Armstrong D, *et al.* The effect of ammonia on omeprazole-induced reduction of gastric acidity in subjects with Helicobacter pylori infection. *Am J Gastroenterol* 2000;**95**:947–55.
8 **Gillen D**, Wirz AA, McColl KE. Helicobacter pylori eradication releases prolonged increased acid secretion following omeprazole treatment. *Gastroenterology* 2004;**126**:980–8.
9 **Labenz J**, Blum AL, Bayerdorffer E, *et al.* Curing Helicobacter pylori infection in patients with duodenal ulcer may provoke reflux esophagitis. *Gastroenterology* 1997;**112**:1442–7.
10 **Schwizer W**, Thumshirn M, Dent J, *et al.* Helicobacter pylori and symptomatic relapse of gastro-oesophageal reflux disease: a randomised controlled trial. *Lancet* 2001;**357**:1738–42.
11 **Samloff IM**, Varis K, Ihamaki T, *et al.* Relationships among serum pepsinogen I, serum pepsinogen II, and gastric mucosal histology. A study in relatives of patients with pernicious anemia. *Gastroenterology* 1982;**83**:204–9.
12 **Karnes WE Jr**, Samloff IM, Siurala M, *et al.* Positive serum antibody and negative tissue staining for Helicobacter pylori in subjects with atrophic body gastritis. *Gastroenterology* 1991;**101**:167–74.
13 **Tucci A**, Poli L, Tosetti C, *et al.* Reversal of fundic atrophy after eradication of Helicobacter pylori. *Am J Gastroenterol* 1998;**93**:1425–31.
14 **Satoh K**, Kimura K, Takimoto T, *et al.* A follow-up study of atrophic gastritis and intestinal metaplasia after eradication of Helicobacter pylori. *Helicobacter* 1998;**3**:236–40.
15 **Farinati F**, Foschia F, Di Mario F, *et al.* H. pylori eradication and gastric precancerous lesions. *Gastroenterology* 1998;**115**:512–14.
16 **van der Hulst RW**, van der Ende A, Dekker FW, *et al.* Effect of Helicobacter pylori eradication on gastritis in relation to cagA: a prospective 1-year follow-up study. *Gastroenterology* 1997;**113**:25–30.
17 **Annibale B**, Aprile MR, D'Ambra G, *et al.* Cure of Helicobacter pylori infection in atrophic body gastritis patients does not improve mucosal atrophy but reduces hypergastrinemia and its related effects on body ECL-cell hyperplasia. *Aliment Pharmacol Ther* 2000;**14**:625–34.
18 **Morris A**, Nicholson G. Ingestion of Campylobacter pyloridis causes gastritis and raised fasting gastric pH. *Am J Gastroenterol* 1987;**82**:192–9.
19 **Gooz M**, Hammond CE, Larsen K, *et al.* Inhibition of human gastric H(+)-K(+)-ATPase alpha-subunit gene expression by Helicobacter pylori. *Am J Physiol Gastrointest Liver Physiol* 2000;**278**:G981–91.
20 **Smolka AJ**, Larsen KA, Hammond CE. Location of a cytoplasmic epitope for monoclonal antibody HK 12.18 on H,K-ATPase alpha subunit. *Biochem Biophys Res Commun* 2000;**273**:942–7.
21 **Chittajallu RS**, Dorrian CA, Neithercut WD, *et al.* Is Helicobacter pylori associated hypergastrinaemia due to the bacterium's urease activity or the antral gastritis? *Gut* 1991;**32**:1286–90.
22 **Beales IL**, Calam J. Inhibition of carbachol stimulated acid secretion by interleukin 1beta in rabbit parietal cells requires protein kinase C. *Gut* 2001;**48**:782–9.
23 **Takashima M**, Furuta T, Hanai H, *et al.* Effects of Helicobacter pylori infection on gastric acid secretion and serum gastrin levels in Mongolian gerbils. *Gut* 2001;**48**:765–73.
24 **Robert A**, Olafsson AS, Lancaster C, *et al.* Interleukin-1 is cytoprotective, antisecretory, stimulates PGE2 synthesis by the stomach, and retards gastric emptying. *Life Sci* 1991;**48**:123–34.
25 **Wallace JL**, Cucala M, Mugridge K, *et al.* Secretagogue-specific effects of interleukin-1 on gastric acid secretion. *Am J Physiol* 1991;**261**:G559–64.
26 **Tache Y**, Saperas E. Potent inhibition of gastric acid secretion and ulcer formation by centrally and peripherally administered interleukin-1. *Ann N Y Acad Sci* 1992;**664**:353–68.
27 **Cave DR**, Vargas M. Effect of a Campylobacter pylori protein on acid secretion by parietal cells. *Lancet* 1989;**2**:187–9.
28 **Hoffman JS**, King WW, Fox JG, *et al.* Rabbit and ferret parietal cell inhibition by Helicobacter species. *Dig Dis Sci* 1995;**40**:147–52.
29 **Pfeiffer A**, Rochlitz H, Noelke B, *et al.* Muscarinic receptors mediating acid secretion in isolated rat gastric parietal cells are of M3 type. *Gastroenterology* 1990;**98**:218–22.
30 **Sandor A**, Kidd M, Lawton GP, *et al.* Neurohormonal modulation of rat enterochromaffin-like cell histamine secretion. *Gastroenterology* 1996;**110**:1084–92.
31 **Aihara T**, Fujishita T, Kanatani K, *et al.* Impaired gastric secretion and lack of trophic responses to hypergastrinemia in M3 muscarinic receptor knockout mice. *Gastroenterology* 2003;**125**:1774–84.
32 **Paradiso AM**, Townsley MC, Wenzl E, *et al.* Regulation of intracellular pH in resting and in stimulated parietal cells. *Am J Physiol* 1989;**257**:C554–61.
33 **Stuart-Tilley A**, Sardet C, Pouyssegur J, *et al.* Immunolocalization of anion exchanger AE2 and cation exchanger NHE-1 in distinct adjacent cells of gastric mucosa. *Am J Physiol* 1994;**266**:C559–68.
34 **Furuta T**, Baba S, Takashima M, *et al.* H+/K+-adenosine triphosphatase mRNA in gastric fundic gland mucosa in patients infected with Helicobacter pylori. *Scand J Gastroenterol* 1999;**34**:384–90.
35 **Iijima K**, Sekine H, Koike T, *et al.* Long-term effect of Helicobacter pylori eradication on the reversibility of acid secretion in profound hypochlorhydria. *Aliment Pharmacol Ther* 2004;**19**:1181–8.

Available online at www.sciencedirect.com
SCIENCE DIRECT®
Biochemical and Biophysical Research Communications 340 (2006) 742–750
BBRC
www.elsevier.com/locate/ybbrc

Angiotensin II promotes the proliferation of activated pancreatic stellate cells by Smad7 induction through a protein kinase C pathway

Kouji Hama [a], Hirohide Ohnishi [a,*], Hiroyoshi Aoki [a], Hiroto Kita [a], Hironori Yamamoto [a], Hiroyuki Osawa [a], Kiichi Sato [a], Kiichi Tamada [a], Hirosato Mashima [b], Hiroshi Yasuda [c], Kentaro Sugano [a]

[a] *Department of Gastroenterology, Jichi Medical School, Tochigi 329-0498, Japan*
[b] *Department of Gastroenterology, University of Tokyo School of Medicine, Tokyo 113-8655, Japan*
[c] *Division of Gastroenterology, Showa University Fujigaoka Hospital, Kanagawa 227-8501, Japan*

Received 28 November 2005
Available online 20 December 2005

Abstract

Activated pancreatic stellate cells (PSCs) play major roles in promoting pancreatic fibrosis. We previously reported that angiotensin II (Ang II) enhances activated PSC proliferation through EGF receptor transactivation. In the present study, we elucidated a novel intracellular mechanism by which Ang II stimulates cellular proliferation. TGF-β_1 inhibits activated PSC proliferation via a Smad3 and Smad4-dependent pathway in an autocrine manner. We demonstrated that Ang II inhibited TGF-β_1-induced nuclear accumulation of Smad3 and Smad4. Furthermore, Ang II rapidly induced inhibitory Smad7 mRNA expression. Adenovirus-mediated Smad7 overexpression inhibited TGF-β_1-induced nuclear accumulation of Smad3 and Smad4, and potentiated activated PSC proliferation. PKC inhibitor Go6983 blocked the induction of Smad7 mRNA expression by Ang II. In addition, 12-*O*-tetradecanoyl-phorbol 13-acetate, a PKC activator, increased Smad7 mRNA expression. These results suggest that Ang II enhances activated PSC proliferation by blocking autocrine TGF-β_1-mediated growth inhibition by inducing Smad7 expression via a PKC-dependent pathway.

Keywords: Angiotensin II; Pancreatic stellate cell; Proliferation; Smad; TGF-β; Protein kinase C; NF-κB

Pancreatic stellate cells (PSCs) were recently identified and characterized [1]. In the normal pancreas, PSCs possess fat droplets containing vitamin A and are quiescent. In the quiescent state, they are characterized by desmin positive but α-smooth muscle actin (α-SMA) negative staining [1]. When cultured in vitro, PSCs are auto-activated (auto-transformed) changing their morphological and functional features [2]. PSCs start losing vitamin A containing lipid droplets, highly proliferating, increasing expression of α-SMA, and producing and secreting extracellular matrix components such as collagen and fibronectin. That is, PSCs are auto-transformed to myofibroblast-like cells. In vivo, PSCs are also activated during pancreatic fibrosis [3]. Thus, activated PSCs are believed to play a central role in pancreatic fibrosis.

Ang II is an octapeptide that causes diverse physiological and pathological actions on cardiovascular systems. It regulates blood pressure and the homeostasis of salts and potassium by acting on vascular smooth muscle, the kidney, and the adrenal gland [4]. Ang II also acts as a growth factor on myocytes and myofibroblasts in pathological conditions, such as remodeling and fibrosis of the heart after chronic hypertension and myocardial infarction [5]. Ang II has also been recently shown to play important roles in fibrosis in extra-cardiovascular organs. For example, Ang II promotes pulmonary fibrosis after lung injury [6] and also mediates hepatic fibrosis after chronic liver

* Corresponding author. Fax: +81 285 44 8297.
E-mail address: hohnishi@jichi.ac.jp (H. Ohnishi).

0006-291X/$ - see front matter © 2005 Elsevier Inc. All rights reserved.
doi:10.1016/j.bbrc.2005.12.069

injury [7]. Chan et al. [8] reported that chronic hypoxia markedly enhanced the expression of angiotensinogen, AT_1 and AT_2 receptors in the pancreas, suggesting that Ang II may play a role in pancreatic chronic injury. Kuno et al. [9] demonstrated that angiotensin converting enzyme inhibitor attenuated pancreatic fibrosis in vivo, further evidence that angiotensin II promotes pancreatic fibrosis. However, the precise mechanism whereby Ang II promotes pancreatic fibrosis remains unresolved. We and others have recently reported that Ang II enhances activated PSC proliferation, suggesting that Ang II promotes pancreatic fibrosis by stimulating activated PSC growth [10,11]. Furthermore, we showed that Ang II enhances activated PSC proliferation by transactivating the EGF receptor [10]. However, blockade of EGF receptor kinase activity did not inhibit the Ang II stimulatory effect on activated PSC proliferation completely. These data suggest another pathway through which Ang II enhances activated PSC proliferation [10].

TGF-β_1 is a major profibrogenic cytokine found in various tissues. Recent evidence suggests that TGF-β is involved in the etiology of pancreatic fibrogenesis, i.e., transgenic mice overexpressing TGF-β_1 in islet cells develop fibrosis of the exocrine pancreas [12]. Inhibition of TGF-β_1 by anti-TGF-β_1 antibody reduced extracellular matrix production in rat cerulein pancreatitis [13]. TGF-β_1 has also been shown to promote PSC activation and collagen production, as well as to inhibit their proliferation in an autocrine fashion [14,15]. In human chronic pancreatitis tissue, TGF-β_1 expression was observed in acinar cells adjacent to areas of fibrosis and in spindle cells in fibrotic bands [3]. Thus, TGF-β_1 may promote pancreatic fibrosis, in part, by modulating PSC functions.

Sma- and Mad-related proteins (Smads) are a group of recently identified molecules that function as intracellular signaling mediators and modulators of TGF-β family members [16]. Smads can be classified into three groups: receptor-regulated Smads (R-Smads), common mediator Smad (Co-Smads), and inhibitory Smads (I-Smad). In the TGF-β signaling pathway, Smad 2 and Smad 3 function as R-Smads, Smad 4 as a Co-Smad, and Smad 7 as an I-Smad. Upon TGF-β binding to TGF-β type II receptor, the type II receptor kinase phosphorylates the GS domain of TGF-β type I receptor, leading to its activation. The activated type I receptor kinase phosphorylates Smad2 and Smad3 (R-Smads) at two serine residues in the SSXS motif at their extreme C termini [17,18]. Phosphorylated Smad2 and Smad3 form oligomeric complexes with Smad4 (Co-Smad), which subsequently translocate into the nucleus and activate the transcription of target genes. Smad7 acts in opposition to the signal-transducing R- and Co-Smads by forming stable associations with activated type-I receptors, thus preventing the phosphorylation of R-Smads [19,20]. We recently reported that autocrine TGF-β_1 inhibits PSC proliferation via a Smad3-dependent pathway [21].

Interactions between TGF-β/Smad signaling and other signaling systems have been reported [22]. However, interaction between Ang II and TGF-β signaling pathways is poorly defined. In this study, we hypothesized that Ang II attenuates TGF-β_1-induced growth inhibition of activated PSCs and consequently, enhances activated PSC proliferation via a novel pathway. We demonstrate that Ang II inhibits TGF-β_1-induced nuclear accumulation of Smad3 and Smad4. We also show that Ang II induces the expression of an inhibitory Smad, Smad7. Overexpression of Smad7 attenuated TGF-β_1-induced Smad3 nuclear accumulation and enhances activated PSC proliferation. We also demonstrate that the induction of Smad7 by Ang II is dependent on PKC, but not on NF-κB.

Experimental procedures

Materials. Nycodenz, pronase, and anti-α-SMA antibody were purchased from Sigma (St. Louis, MO); DNase I from Roche (Basel, Switzerland); recombinant human Ang II from Peptide Institute (Osaka, Japan); and collagenase P from Boehringer–Mannheim (Mannheim, Germany). Anti-Smad3-, anti-Smad4, anti-Smad7, and anti-IκB-antibodies were obtained from Santa Cruz (Santa Cruz, CA). Horseradish peroxidase (HRP)-conjugated donkey anti-goat IgG-, HRP-conjugated donkey anti-mouse IgG-, and Cy3-conjugated donkey anti-goat IgG antibodies were purchased from Jackson Immuno Research (West Grove, PA).

Isolation and culture of rat pancreatic stellate cells. Rat pancreatic stellate cells were prepared as described [1]. Briefly, rat pancreata were digested in Gey's balanced salt solution supplemented with 0.05% collagenase P, 0.02% pronase, and 0.1% DNase. After filtration through nylon mesh, cells were centrifuged on a 13.2% Nycodenz gradient at 1400*g* for 20 min. PSCs were collected from the band just above the interface of the Nycodenz solution and the aqueous layer, washed and resuspended in Iscove's modified Dulbecco's medium containing 10% fetal calf serum, 100 U/ml penicillin, and 100 μg/ml streptomycin. PSCs were cultured in a 5% CO_2 atmosphere at 37 °C. All experiments were carried out using PSCs from passages two and three. During these passages, PSCs are culture-activated, transformed to myofibroblast-like cells, and express α-SMA as described previously [21].

Adenovirus infection. Recombinant adenoviruses of Smads and IκB mutant were kindly provided by Dr. Miyazono (University of Tokyo, Japan) and Dr. Iimuro (Hyogo Medical Collage), respectively. We used an adenovirus expressing β-galactosidase (AdLacZ) as an infection control. For a single adenovirus infection, cells were infected with a recombinant adenovirus at a dose of 10 plaque-forming units (pfu) per cell unless otherwise indicated. In the experiments using double adenovirus infection, cells were infected with Smad3 adenovirus (AdSmad3) at a dose of 10 pfu/cell, concomitantly with Smad7 (AdSmad7) or β-galactosidase (AdLacZ) adenoviruses at a dose of 10 pfu/cell.

Immunocytochemistry. Immunocytochemistry was carried out as described previously [21], using an Olympus BX51 microscope (Olympus, Tokyo, Japan). Images were digitized and then processed using the Photoshop 5.0 software (Adobe Systems, Mountain View, CA).

Nuclear extract preparation. Nuclear extracts were prepared by the method of Dignam et al. [23]. After the appropriate treatment, the cells were washed twice with ice-cold PBS, scraped, and resuspended in 400 μl buffer A (10 mM Hepes (pH 7.9), 10 mM KCl, 0.1 mM EDTA, 0.1 mM EGTA, 1 mM dithiothreitol, and 0.5 mM PMSF). After 15 min, Nonidet P-40 was added to a final concentration of 0.6%. Nuclei were pelleted and resuspended in 50 μl buffer B (20 mM Hepes (pH 7.9), 0.4 M NaCl, 1 mM EDTA, 1 mM EGTA, 1 mM dithiothreitol, and 1 mM PMSF). After incubation at 4 °C for 30 min, the lysate was centrifuged, and the supernatant containing the nuclear proteins was transferred to new vials. The protein concentration of the extract was measured using a Bio-Rad Protein Determination kit (Hercules, CA).

Western blotting. Western blotting was carried out as described previously [24], using the enhanced chemiluminescence reagent to visualize

the secondary antibody. For gel electrophoresis, 10 μg protein was loaded on each lane of a 10% sodium dodecyl sulfate–polyacrylamide gel.

Measurement of DNA synthesis. DNA synthesis was measured by determining the amount of [^{3}H]thymidine incorporation into cells. After [^{3}H]thymidine was added to the culture medium, the cells were incubated for 2 h and [^{3}H]thymidine incorporation was measured as described previously [25].

Statistical analysis. The data were analyzed by ANOVA to determine statistical significance and $P < 0.05$ was considered significant.

Results

Ang II inhibited Smad3 and Smad4 nuclear accumulation in PSCs and blocked TGF-β_1 inhibitory effect on PSC proliferation

In order to examine possible Ang II interference with the TGF-β_1 signaling pathway, we first investigated the effect of exogenous TGF-β_1 on the DNA synthesis in activated PSCs. As shown in Fig. 1, TGF-β_1 added into the culture medium inhibited the DNA synthesis in PSCs. Maximum inhibition was observed at 30 pM. Therefore, we utilized 30 pM TGF-β_1 in the further experiments. Since a dose of 100 nM Ang II maximally enhances PSC proliferation [10], this dosage was employed for all experiments. We then investigated the effect of Ang II on TGF-β_1-induced Smad3 and Smad4 nuclear accumulation in activated PSCs using immunocytochemistry. Smad3 is known to mediate the TGF-β_1 inhibitory effect on PSC proliferation [21]. As shown in Fig. 2, untreated PSCs showed diffuse cytoplasmic staining for Smad3, and only nuclear bodies were stained in their nuclei (Fig. 2A, arrows). When stimulated with 30 pM TGF-β_1, nuclear staining of Smad3 was exclusively detectable in PSCs (Fig. 2B). In contrast, cells pretreated with Ang II prior to adding TGF-β_1 showed only the nuclear body staining for Smad3 in their nuclei (Fig. 2C, arrows), indicating that Ang II suppressed the TGF-β_1-induced nuclear translocation of Smad3. In addition, untreated PSCs showed diffuse cytoplasmic staining for Smad4, but nuclear staining was barely observed (Fig. 2D). When stimulated with 30 pM TGF-β_1, nuclear staining of Smad4 was exclusively detectable in PSCs (Fig. 2E, arrowheads). However, cells pretreated with Ang II prior to adding TGF-β_1 showed cytoplasmic but not nuclear staining for Smad4 (Fig. 2F), indicating that Ang II also suppressed the TGF-β_1-induced nuclear translocation of Smad4.

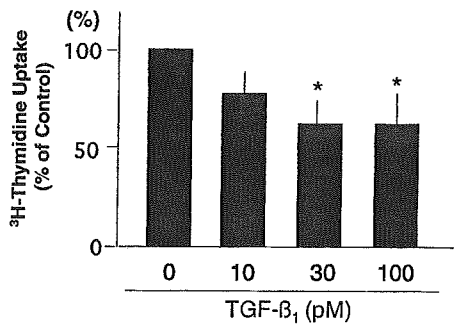

Fig. 1. TGF-β_1 inhibits activated PSC proliferation. Cells were incubated with the indicated amounts of TGF-β_1 added in the culture medium for 48 h, followed by the determination of the DNA synthesis using [^{3}H]thymidine incorporation assay. Values are means ± SE for three independent experiments. *$P < 0.05$ vs. control.

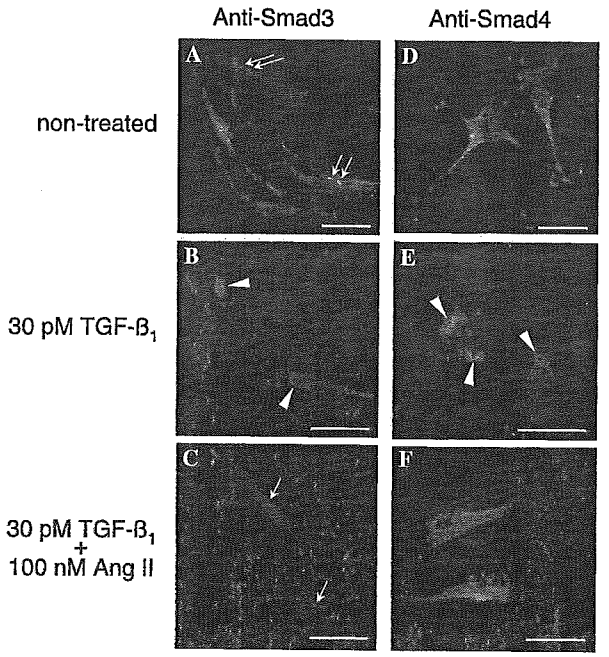

Fig. 2. Ang II inhibited TGF-β_1-induced nuclear accumulation of Smad3 and Smad 4. Activated PSCs were incubated in the presence or absence of 100 nM Ang II for 48 h, followed by the stimulation with 30 pM TGF-β_1 for 2 h. Then, nuclear accumulation of Smad3 and Smad4 was examined using immunocytochemistry with anti-Smad3 (A–C) or anti-Smad4 (D–F) antibodies. The results shown are representative of three independent experiments. Bars, 10 μm.

For more quantitative evaluation of TGF-β_1-induced nuclear accumulation of Smad3 and Smad4, we examined the effect of Ang II on TGF-β_1-induced Smad3 and Smad4 nuclear accumulation using Western blotting of nuclear extracts. Since the level of endogenously expressed Smad3 protein in PSCs is below the sensitivity of Western blots, we employed adenovirus-mediated overexpression of Smad3. We previously reported that more than 98% of the PSCs are infected with various Smads expressing adenovirus vectors and each Smad protein was sufficiently expressed to permit detection [21]. The expression of endogenous Smad4 protein in PSCs is sufficient to permit detection by Western blotting, i.e., in the absence of adenovirus-mediated overexpression. As shown in Fig. 3, 30 pM TGF-β_1 increased Smad3 and Smad4 nuclear accumulation in activated PSCs (Fig. 3, top and bottom panels; first and second lanes). In contrast, pretreatment of PSCs with 100 nM Ang II attenuated TGF-β_1-induced Smad3 and Smad4 nuclear accumulation (Fig. 3A, top and bottom panels; third and fourth lanes). However, the amount of overexpressed Smad3 protein in whole cell lysates is

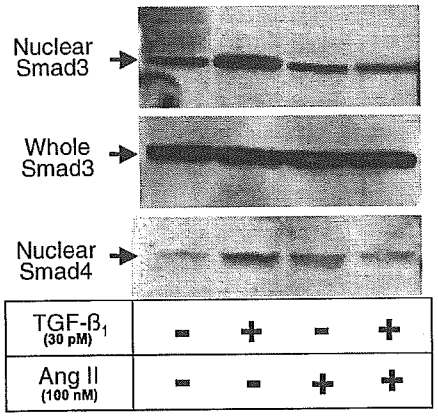

Fig. 3. Ang II inhibited TGF-β_1-induced nuclear accumulation of overexpressed Smad3 and endogenous Smad4 in activated PSCs. Twenty-four hour post-AdSmad3-infected PSCs were incubated with or without 100 nM Ang II for 48 h followed by either 30 pM TGF-β_1 in the culture medium for 24 h or the cells left untreated. Nuclear accumulation of Smad3 (top panel) and Smad4 (bottom panel) was analyzed with Western blotting of nuclear extracts using specific antibodies. Confirmation of equivalent Smad3 overexpression by AdSmad3 infection in each sample was provided by Western blotting of whole cell lysate using an anti-Smad3 antibody (middle panel). The results shown are representative of three independent experiments.

identical under all experimental conditions (Fig. 3, middle panel). These observations reinforce that Ang II attenuates Smad3 and Smad4 nuclear accumulation induced by TGF-β_1 in PSCs. Furthermore, 100 nM Ang II blocked the 30 pM TGF-β_1 inhibitory effect on PSC proliferation (Fig. 4, second third columns). Cumulatively, these data suggest that Ang II enhances PSC proliferation by blocking TGF-β_1 inhibition of PSC proliferation by inhibiting Smad3 and Smad4 nuclear accumulation.

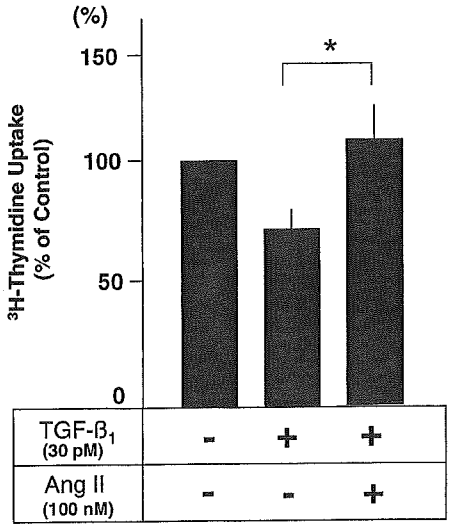

Fig. 4. Ang II blocked TGF-β_1 inhibition of activated PSC proliferation. Activated PSCs were incubated in the presence or absence of 100 nM Ang II of 48 h, followed by the stimulation with 30 pM TGF-β_1 for 24 h. Then, DNA synthesis was determined using [^{3}H]thymidine incorporation assay. The values are expressed as means ± SE for three independent experiments. *$P < 0.05$.

Ang II enhanced Smad7 mRNA expression in PSCs

Down-regulation of TGF-β signaling occurs via a feedback mechanism involving the induction of the inhibitory Smad7, which in turn, blocks TGF-β-induced growth inhibition. Interferon-γ was recently shown to inhibit TGF-β_1/Smad signaling via the induction of Smad7 expression [26]. Therefore, we hypothesized that Smad7 plays a role in Ang II-induced suppression of TGF-β_1/Smad3/4 signaling. As shown in Fig. 5, 100 nM Ang II increased the level of Smad7 mRNA expression within 1 h and reached a maximum level after 2 h of exposure.

Adenovirus-mediated Smad7 overexpression inhibited Smad3 and Smad4 nuclear accumulation and enhanced PSC proliferation

We next determined whether or not Ang-II-induced Smad7 expression can block TGF-β_1 signaling. We examined the effect of adenovirus-mediated Smad7 overexpression on Smad3 and Smad4 nuclear accumulation in PSCs, using immunocytochemistry. We utilized an adenovirus expressing β-galactosidase (AdLacZ) as an infection control. As shown in Fig. 6A, Smad7 protein signal was observed in more than 98% PSCs infected with AdSmad7 (Fig. 6A, panels a and c). In contrast, Smad7 signal was barely detected in cells infected with AdLacZ (Fig. 6A, panels b and d). These data indicate that infection with AdSmad7-induced Smad7 overexpression in activated PSCs. As shown in Fig. 5B, PSCs infected with AdLacZ showed diffuse cytoplasmic staining for Smad3, and only nuclear bodies were stained in their nuclei (Fig. 6B, panel a, arrow heads). When stimulated with 30 pM TGF-β_1, nuclear staining of Smad3 was exclusively detectable in PSCs infected with AdLacZ (Fig. 6B, panel b, arrows). In contrast, cells infected with AdSmad7 showed only the nuclear body staining for Smad3 in their nuclei after TGF-β_1 stimulation (Fig. 6B, panel c, arrow heads), indicating that Smad7 overexpression induced by AdSmad7 infection suppressed the TGF-β_1-induced nuclear translocation

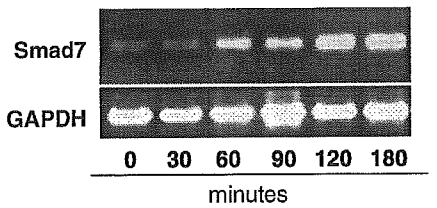

Fig. 5. Ang II increased Smad7 mRNA expression in PSCs. PSCs were incubated for indicated times with 100 nM Ang II. After incubation, Smad7 mRNA expression was determined by RT-PCR, using glyceraldehyde-3-phosphate dehydrogenase (GAPDH) mRNA expression as a control.

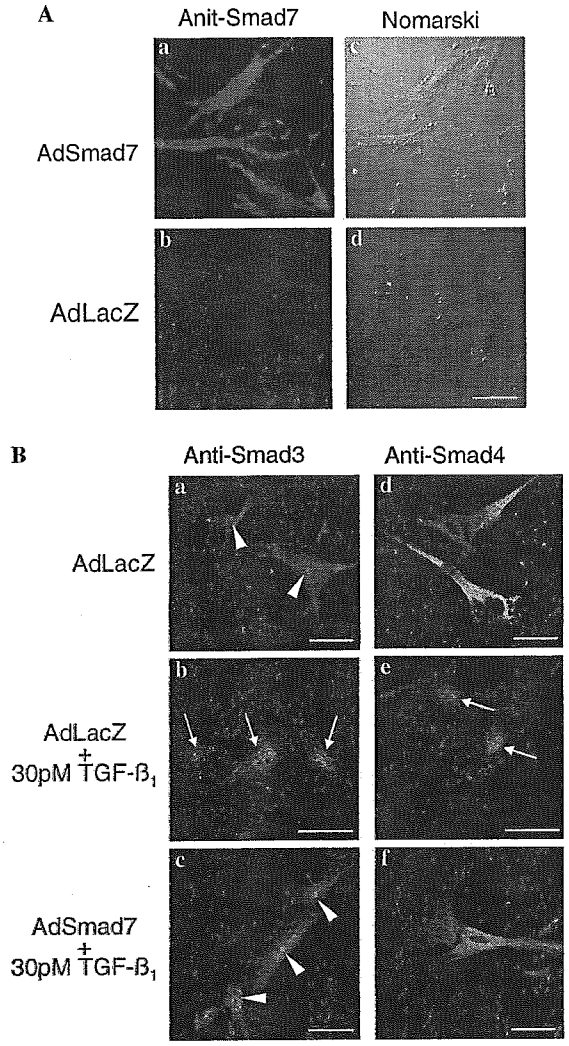

Fig. 6. Smad7 overexpression inhibited TGF-β_1-induced nuclear accumulation of Smad3 and Smad4 in activated PSCs. Activated PSCs were infected with AdSmad7 (A: a and c, B: c and f) or AdLacZ (A: b and d, B: a b, d, and e). (A) Activated PSCs infected with AdSmad7 (a and c) or AdLacZ (b and d) were immunostained with anti-Smad7 antibody 48 h after the infection (a and b). Panels c and d are Nomarski images corresponding to panels a and b, respectively. (B) Forty-eight hour post-AdSmad7 or post-AdLacZ-infected PSCs were incubated for 2 h with (b, c, e, and f) or without (a,d) 30 pM TGF-β_1. Nuclear accumulation of Smad3 and Smad4 was examined using immunocytochemistry with anti-Smad3 (a–c) or anti-Smad4 (d–f) antibodies. The results shown are representative of three independent experiments. Bars, 10 μm.

of Smad3. In addition, PSCs infected with AdLacZ showed diffuse cytoplasmic staining for Smad4, but nuclear staining was barely observed (Fig. 6B, panel d). When stimulated with 30 pM TGF-β_1, nuclear staining of Smad4 was exclusively detectable in PSCs infected with LacZ (Fig. 6B, panel e, arrows). However, cells infected with AdSmad7 showed cytoplasmic but not nuclear staining for Smad4 (Fig. 6B, panel f), indicating that Smad7 overexpression also suppressed the TGF-β_1-induced nuclear translocation of Smad4. These data suggest that Smad7 overexpression inhibits the initial event in the TGF-β_1/Smad signaling of TGF-β_1 inhibition of PSC proliferation. For more quantitative analysis, we examined the effect of Smad7 overexpression on Smad3 and Smad 4 nuclear accumulation using Western blotting. Since the level of endogenously expressed Smad3 protein in PSCs is below the sensitivity of Western blots as described above, we again utilized activated PSCs infected with AdSmad3. Smad3 protein was overexpressed equally with AdSmad3 infection under all conditions (Fig. 7, second panel). In control cells infected with AdLacZ, 30 pM of exogenous TGF-β_1-induced Smad3 and Smad4 nuclear accumulation (Fig. 7, first and third panels, first and second lanes). On the contrary, in AdSmad7-infected cells overexpressing Smad7, exogenous TGF-β_1-stimulated nuclear accumulation of Smad3 and Smad4 was inhibited (Fig. 7, first and third panels, third and fourth lanes). These data reinforce that Smad7 overexpression inhibits Smad3/4-dependent TGF-β_1 signaling pathway in activated PSCs. We subsequently investigated the effect of Smad7 overexpression on PSC proliferation. As shown in Fig. 8A, infection with AdSmad7 markedly enhanced PSC proliferation. Enhanced cell proliferation occurred concomitantly with the overexpression of Smad7 protein (Fig. 8B, Western blotting). AdSmad7 infection enhanced PSC growth to a similar extent to that by angiotensin II as shown previously [10]. In contrast, infection with AdLacZ did not alter PSC proliferation (Fig. 8A).

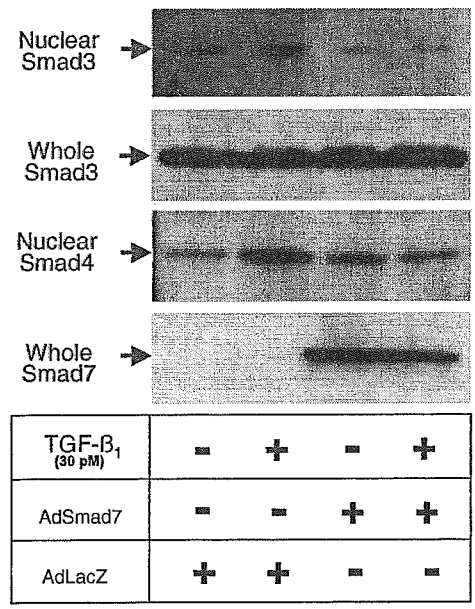

Fig. 7. Smad7 overexpression inhibited nuclear accumulation of overexpressed Smad3 and endogenous Smad4 induced by TGF-β_1. Activated PSCs were infected with AdSmad3 in combination with AdLacZ (first and second lanes) or AdSmad7 (third and fourth lanes). Forty-eight hours after the infection, cells were incubated with (second and fourth lanes) or without (first and third lanes) 30 pM TGF-β_1 for 2 h. Nuclear accumulation of Smad3 (top panel) and Smad4 (third panel) was analyzed by Western blotting of nuclear extracts using their specific antibodies. Equal expression of Smad3 (second panel) and Smad7 (fourth panel) following adenovirus infection was confirmed by Western blotting of whole lysate. The results shown are representative of three independent experiments.

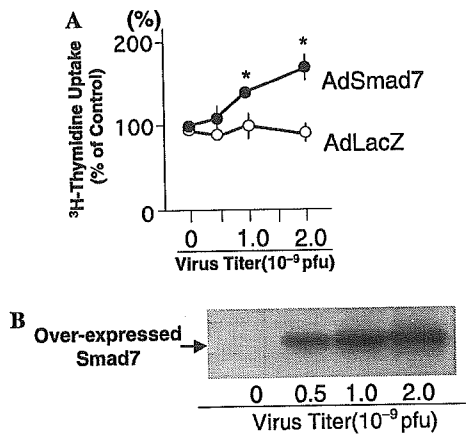

Fig. 8. Smad7 overexpression enhanced DNA synthesis in PSCs. (A) PSCs were infected with AdSmad7 (closed circles) or AdLacZ (open circles) at indicated doses. After 48 h of incubation, DNA synthesis was determined using a [^{3}H]thymidine incorporation assay. The values are expressed as means ± SE for three independent experiments. *$P < 0.05$ vs. control. (B) Dose-dependent Smad7 overexpression by AdSmad7 infection was confirmed by Western blotting of PSC whole lysates 48 h after the infection using an anti-Smad7 antibody.

These data suggest that Smad7 overexpression following AdSmad7 infection mimics both the Ang II inhibitory effect on TGF-β_1 signaling in PSCs and Ang II enhancement of PSC proliferation.

Ang II-induced Smad7 expression via PKC dependent but NF-κB independent pathway

We attempted to elucidate the intracellular signaling pathway by which Ang II induces Smad7 expression. Since NF-κB transcription factor is known to mediate Smad7 induction by various cytokines [27], we examined NF-κB involvement in Smad7 induction by Ang II, using an adenovirus expressing an HA-tagged IκB mutant (Ad5IκB) that contained serine-to-alanine mutations in residues 32 and 36 [28]. This IκB mutant functions as an IκB super-repressor. The expression of the HA-tagged IκB mutant in PSCs after Ad5IκB infection was confirmed by its slower mobility on Western blots in comparison to endogenous IκB (Fig. 9A). In control experiments, the suppression of NF-κB function by the HA-tagged IkB mutant was examined by assessing the effect of Ad5IκB infection on interleukin-1β-induced ICAM-1 expression, which is mediated by NF-κB in PSCs [29]. We also used a β-galactosidase expressing adenovirus (AdLacZ) as an infection control. As shown in Fig. 9B, interleukin-1β increased ICAM-1 mRNA expression in AdLacZ-infected PSCs, whereas interleukin-1β failed to induce it in Ad5IκB-infected PSCs, suggesting that the expression of the HA-tagged IκB mutant after Ad5IκB infection blocks the NF-κB-dependent signaling pathway in PSCs. In contrast, Ang II successfully enhanced Smad7 mRNA expression in both AdLacZ- and Ad5IκB-infected PSCs (Fig. 9C). These data suggest that Ang II induces Smad7 mRNA expression via a NF-κB-independent pathway.

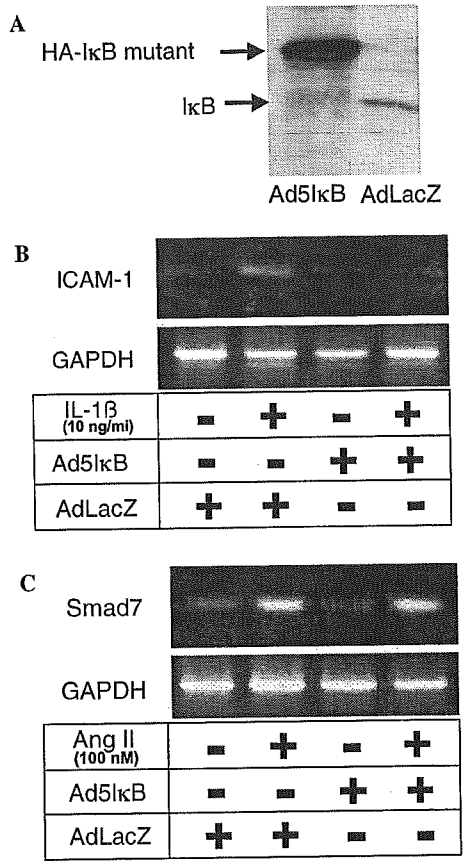

Fig. 9. Smad7 induction by Ang II is independent of NF-κB transcription factor. PSCs were infected with either AdLacZ or Ad5IκB. (A) Expression of HA-tagged IκB mutant was assessed by Western blotting of whole lysate using an anti-IκB antibody. (B,C) Forty-eight hours after infection, PSCs were incubated in the presence or absence of 10 ng/ml IL-1β (B) or 100 nM Ang II (C) for 2 h, then ICAM-1 (B) or Smad7 (C) mRNA expression was determined by RT-PCR, using GAPDH mRNA expression as a control.

Recently, it was reported that Smad7 expression is regulated via a PKC-dependent pathway in some types of cells [30]. In addition, Ang II is known to activate PKC in various cells. Therefore, we hypothesized that Smad7 induction by Ang II may be dependent on PKC. In order to examine this hypothesis, we blocked PKC with a PKC inhibitor Go6983. When PSCs are pretreated with Go6983, a 100 nM dose of Ang II did not enhance Smad7 mRNA expression (Fig. 10A). Moreover, 12-*O*-tetradecanoyl-phorbol 13-acetate, a PKC activator, increased Smad7 mRNA expression (Fig. 10B). These data strongly suggest that Ang II induces Smad7 mRNA expression via a PKC-dependent pathway.

Discussion

In this study, we report a novel mechanism for enhancing activated PSC proliferation by Ang II. Both Ang II and the overexpression of Smad 7 inhibited TGF-β_1-stimulated nuclear accumulation of Smad3 and Smad4 concomitantly

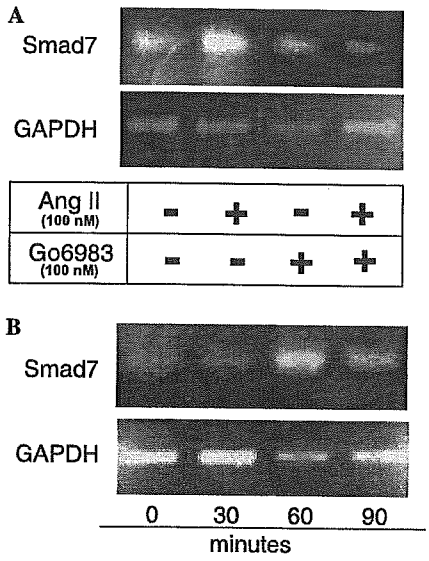

Fig. 10. Smad7 induction by Ang II is dependent on PKC. (A) PSCs were pretreated with 60 nM PKC inhibitor Go6983 for 1 h and then incubated with 100 nM Ang II for 2 h. (B) Cells were incubated with 100 nM TPA for indicated times. After the incubation, Smad7 mRNA was examined with RT-PCR, using GAPDH mRNA expression as a control (A,B).

with the enhanced proliferation of activated PSC. Ang II and TPA increased Smad7 mRNA expression. Furthermore, the PKC inhibitor, Go6983, prevented enhanced Smad7 mRNA expression by Ang II. Accordingly, Ang II enhances activated PSC proliferation by attenuating the autocrine TGF-β_1 inhibitory effect via Smad7 induction and, it appears as if PKC is involved in this mechanism.

Since Ang II is a physiological peptide that regulates blood pressure and the homeostasis of the cardiovascular system, its pathological role in tissue fibrosis has been studied extensively in cardiovascular organs. In pathological conditions, such as remodeling of the heart after chronic hypertension and myocardial infractions, Ang II promotes cardiac fibrosis by acting as a growth factor for myofibroblasts. In the kidney, Ang II induces the proliferation of mesangial cells and fibroblasts, and consequently promotes renal fibrosis [31]. The transactivation of the EGF-receptor leading to the activation of mitogen-activated protein kinases is a well-documented event in the Ang II intracellular signaling pathway that contributes to cellular growth [32]. Our recent report that Ang II stimulates activated PSC proliferation by transactivating the EGF-receptor leading to ERK activation suggests that Ang II promotes pancreatic fibrosis by enhancing activated PSC growth [10]. Ang II increased DNA synthesis in activated PSCs concomitant with activating the EGF-receptor and its downstream ERK. Moreover, the EGF-receptor kinase inhibitor AG1478 blocked Ang-II-induced ERK activation, and inhibited Ang-II-stimulated DNA synthesis by approximately 50% [10]. Although these data suggest that Ang II stimulates PSC proliferation via an EGF-receptor transactivation-ERK pathway, the 50% inhibition of Ang-II-enhanced PSC proliferation by an EGF-receptor kinase inhibitor suggests the existence of an alternate intracellular signaling pathway for the Ang II mitogenic effect on PSCs. These observations provided the impetus to conduct the present study in an effort to elucidate this novel signaling pathway for the Ang II mitogenic effect on activated PSCs.

TGF-β_1 promotes PSC activation and collagen production, but inhibits PSC proliferation [14,15]. We previously elucidated the signaling pathways by which autocrine TGF-β_1 regulates PSC functions [21]. We have shown that TGF-β_1 stimulates PSC activation and inhibits its proliferation via Smad2-dependent and Smad3-dependent pathways, respectively. In the current study, we evaluated the effect of Ang II on Smad3 and Smad4 nuclear accumulation (Figs. 2 and 3). Although Ang II inhibits TGF-β-induced Smad2 nuclear accumulation in PSCs, it does not modulate PSC activation (unpublished data). These observations warranted further study on the role of the Ang II inhibitory effect on TGF-β-induced Smad2 nuclear accumulation in the regulation of PSC functions.

Both Ang II and TGF-β_1 play important roles in tissue fibrogenesis and their interaction in this process has recently been described. Ang II upregulates the expression of one of the TGF-β receptors, endoglin, in cardiac fibroblasts [33]. Upregulated endoglin modulates the Ang II profibrotic effects by increasing type1-collagen expression. Furthermore, in vivo studies have shown that Ang II infusion increases TGF-β_1 mRNA expression in vascular smooth muscle and myofibroblast-like cells [34]. Therefore, considerable attention has been directed to the positive interplay between Ang-II and TGF-β_1 in the etiology of tissue fibrogenesis. In the present study, we provide the first evidence documenting an AngII inhibitory effect on the TGF-β/Smad signaling pathway and its subsequent effects on activated PSC proliferation.

Two inhibitory Smads, Smad6, and Smad7, have been identified and characterized in this TGF-β signaling system. Smad6 functions as an I-Smad in the BMP signaling pathway [35], whereas Smad7 inhibits all TGF-β family signaling pathways [19,20]. Therefore, we investigated the role of Smad7 in the AngII-TGF-β interplay regulating PSC proliferation. Since TGF-β induces Smad7 expression in various cell types, Smad7 is considered to act in a negative-feedback regulation of TGF-β family stimulation. Other pro-inflammatory cytokines, such as TNF-α, IL-1β [27] and IFN-γ [26], have recently been shown to induce Smad7 expression. Smad7 induction by TNF-α and IL-β is mediated by an NF-κB-dependent pathway [27]. IFN-γ induces Smad7 expression via a JAK-Stat signaling pathway [26], however, the PKC activator, TPA, has been shown to increase Smad7 expression in lung fibroblasts, suggesting PKC involvement in Smad7 induction [30]. Nevertheless, the cytokine that induces Smad7 expression via a PKC-dependent pathway has not been identified. Ang II is known to activate PKC and NF-κB. Therefore, we examined the roles of NF-κB and PKC in the AngII/

Smad7 induction pathway and showed that Smad7 induction is PKC-dependent, but NF-κB independent. Thus, Ang II is the first cytokine shown to induce Smad7 expression via a PKC-dependent pathway.

In conclusion, we have shown that Ang II enhances the proliferation of activated PSC by attenuating the autocrine TGF-β_1 inhibitory effect by Smad7 induction via a PKC-dependent pathway. These observations provide new and important data for understanding the mechanism of pancreatic fibrosis.

Acknowledgments

We are grateful to Dr. Miyazono (University of Tokyo) and Dr. Iimuro (Hyogo Medical College) for Smads and IκB mutant adenovirus vectors, respectively. This work was supported by Grants-in-Aid from the ministry of Education, Culture, Sports, Science and Technology of Japan.

References

[1] M.V. Apte, P.S. Haber, T.L. Applegate, I.D. Norton, G.W. McCaughan, M.A. Korsten, R.C. Pirola, J.S. Wilson, Periacinar stellate shaped cells in rat pancreas: identification, isolation, and culture, Gut 43 (1998) 128–133.

[2] M.G. Bachem, E. Schneider, H. Gross, H. Weidenbach, R.M. Schmid, A. Menke, M. Siech, H. Beger, A. Grunert, G. Adler, Identification, culture, and characterization of pancreatic stellate cells in rats and humans, Gastroenterology 115 (1998) 421–432.

[3] P.S. Haber, G.W. Keogh, M.V. Apte, C.S. Moran, N.L. Stewart, D.H. Crawford, R.C. Pirola, G.W. McCaughan, G.A. Ramm, J.S. Wilson, Activation of pancreatic stellate cells in human and experimental pancreatic fibrosis, Am. J. Pathol. 155 (1999) 1087–1095.

[4] M.J. Peach, Renin–agiotensin system: biochemistry and mechanisms of action, Physiol. Rev. 57 (1977) 313–370.

[5] K.T. Weber, Y. Sun, L.C. Katwa, Myofibroblasts and local angiotensin II in rat cardiac tissue repair, Int. J. Biochem. Cell Biol. 29 (1997) 31–42.

[6] R.P. Marshall, R.J. McAnulty, G.J. Laurent, Angiotensin II is mitogenic for human lung fibroblasts via activation of the type 1 receptor, Am. J. Respir. Crit. Care Med. 161 (2000) 1999–2004.

[7] J.R. Jonsson, A.D. Clouston, Y. Ando, L.I. Kelemen, M.J. Horn, M.D. Adamson, D.M. Purdie, E.E. Powell, Angiotensin-converting enzyme inhibition attenuates the progression of rat hepatic fibrosis, Gastroenterology 121 (2001) 148–155.

[8] W.P. Chan, M.L. Fung, R. Nobiling, P.S. Leung, Activation of local renin–angiotensin system by chronic hypoxia in rat pancreas, Mol. Cell Endocrinol. 160 (2000) 107–114.

[9] A. Kuno, T. Yamada, K. Masuda, K. Ogawa, M. Sogawa, S. Nakamura, T. Nakazawa, H. Ohara, T. Nomura, T. Joh, T. Shirai, M. Itoh, Angiotensin-converting enzyme inhibitor attenuates pancreatic inflammation and fibrosis in male Wistar Bonn/Kobori rats, Gastroenterology 124 (2003) 1010–1019.

[10] K. Hama, H. Ohnishi, H. Yasuda, N. Ueda, H. Mashima, Y. Satoh, K. Hanatsuka, H. Kita, A. Ohashi, K. Tamada, K. Sugano, Angiotensin II stimulates DNA synthesis of rat pancreatic stellate cells by activating ERK through EGF receptor transactivation, Biochem. Biophys. Res. Commun. 315 (2004) 905–911.

[11] R. Reinehr, S. Zoller, H. Klonowski-Stumpe, C. Kordes, D. Haussinger, Effects of angiotensin II on rat pancreatic stellate cells, Pancreas 28 (2004) 129–137.

[12] M.S. Lee, D. Gu, L. Feng, S. Curriden, M. Arnush, T. Krahl, D. Gurushanthaiah, C. Wilson, D.L. Loskutoff, H. Fox, Accumulation of extracellular matrix and developmental dysregulation in the pancreas by transgenic production of transforming growth factor-beta 1, Am. J. Pathol. 147 (1995) 42–52.

[13] A. Menke, H. Yamaguchi, T.M. Gress, G. Adler, Extracellular matrix is reduced by inhibition of transforming growth factor beta1 in pancreatitis in the rat, Gastroenterology 113 (1997) 295–303.

[14] M.L. Kruse, P.B. Hildebrand, C. Timke, U.R. Folsch, W.E. Schmidt, TGFbeta1 autocrine growth control in isolated pancreatic fibroblastoid cells/stellate cells in vitro, Regul. Pept. 90 (2000) 47–52.

[15] M.V. Apte, P.S. Haber, S.J. Darby, S.C. Rodgers, G.W. McCaughan, M.A. Korsten, R.C. Pirola, J.S. Wilson, Pancreatic stellate cells are activated by proinflammatory cytokines: implications for pancreatic fibrogenesis, Gut 44 (1999) 534–541.

[16] J. Massague, TGF-beta signal transduction, Annu. Rev. Biochem. 67 (1998) 753–791.

[17] M. Macias-Silva, S. Abdollah, P.A. Hoodless, R. Pirone, L. Attisano, J.L. Wrana, MADR2 is a substrate of the TGFbeta receptor and its phosphorylation is required for nuclear accumulation and signaling, Cell 87 (1996) 1215–1224.

[18] X. Liu, Y. Sun, S.N. Constantinescu, E. Karam, R.A. Weinberg, H.F. Lodish, Transforming growth factor beta-induced phosphorylation of Smad3 is required for growth inhibition and transcriptional induction in epithelial cells, Proc. Natl. Acad. Sci. USA 94 (1997) 10669–10674.

[19] H. Hayashi, S. Abdollah, Y. Qiu, J. Cai, Y.Y. Xu, B.W. Grinnell, M.A. Richardson, J.N. Topper, M.A. Gimbrone Jr., J.L. Wrana, D. Falb, The MAD-related protein Smad7 associates with the TGFbeta receptor and functions as an antagonist of TGFbeta signaling, Cell 89 (1997) 1165–1173.

[20] A. Nakao, M. Afrakhte, A. Moren, T. Nakayama, J.L. Christian, R. Heuchel, S. Itoh, M. Kawabata, N.E. Heldin, C.H. Heldin, P. ten Dijke, Identification of Smad7, a TGFbeta-inducible antagonist of TGF-beta signalling, Nature 389 (1997) 631–635.

[21] H. Ohnishi, T. Miyata, H. Yasuda, Y. Satoh, K. Hanatsuka, H. Kita, A. Ohashi, K. Tamada, N. Makita, T. Iiri, N. Ueda, H. Mashima, K. Sugano, Distinct roles of Smad2-, Smad3-, and ERK-dependent pathways in transforming growth factor-{beta}1 regulation of pancreatic stellate cellular functions, J. Biol. Chem. 279 (1994) 8873–8878.

[22] M. Kretzschmar, J. Doody, I. Timokhina, J. Massague, A mechanism of repression of TGFbeta/Smad signaling by oncogenic Ras, Genes Dev. 13 (1999) 804–816.

[23] J.D. Dignam, R.M. Lebovitz, R.G. Roeder, Accurate transcription initiation by RNA polymerase II in a soluble extract from isolated mammalian nuclei, Nucleic Acids Res. 11 (1983) 1475–1489.

[24] H. Ohnishi, S.A. Ernst, D.I. Yule, C.W. Baker, J.A. Williams, Heterotrimeric G-protein Gq/11 localized on pancreatic zymogen granules is involved in calcium-regulated amylase secretion, J. Biol. Chem. 272 (1997) 16056–16061.

[25] C. Kanamaru, H. Yasuda, M. Takeda, N. Ueda, J. Suzuki, T. Tsuchida, H. Mashima, H. Ohnishi, T. Fujita, Smad7 is induced by norepinephrine and protects rat hepatocytes from activin A-induced growth inhibition, J. Biol. Chem. 276 (2001) 45636–45641.

[26] L. Ulloa, J. Doody, J. Massague, Inhibition of transforming growth factor-beta/SMAD signalling by the interferon-gamma/STAT pathway, Nature 397 (1999) 710–713.

[27] M. Bitzer, G. von Gersdorff, D. Liang, A. Dominguez-Rosales, A.A. Beg, M. Rojkind, E.P. Bottinger, A mechanism of suppression of TGF-beta/SMAD signaling by NF-kappa B/RelA, Genes Dev. 14 (2000) 187–197.

[28] Y. Iimuro, T. Nishiura, C. Hellerbrand, K.E. Behrns, R. Schoonhoven, J.W. Grisham, D.A. Brenner, NFkappaB prevents apoptosis and liver dysfunction during liver regeneration, J. Clin. Invest. 101 (1998) 802–811.

[29] A. Masamune, Y. Sakai, K. Kikuta, M. Satoh, A. Satoh, T. Shimosegawa, Activated rat pancreatic stellate cells express intercellular adhesion molecule-1 (ICAM-1) in vitro, Pancreas 25 (2002) 78–85.

[30] H. Tsunobuchi, A. Ishisaki, T. Imamura, Expressions of inhibitory Smads, Smad6 and Smad7, are differentially regulated by TPA in

human lung fibroblast cells, Biochem. Biophys. Res. Commun. 316 (2004) 712–719.
[31] S.A. Mezzano, M. Ruiz-Ortega, J. Egido, Angiotensin II and renal fibrosis, Hypertension 38 (2001) 635–638.
[32] H. Bukhtiar, B.H. Shah, K.J. Catt, A central role of EGF receptor transactivation in angiontensin II-induced cardiac hypertrophy, Trends Pharmacol. Sci. 24 (2003) 239–244.
[33] K. Chen, J.L. Mehta, D. Li, L. Joseph, J. Joseph, Transforming growth factor beta receptor endoglin is expressed in cardiac fibroblasts and modulates profibrogenic actions of angiotensin II, Circ. Res. 95 (2004) 1167–1173.
[34] K. Siato, N. Ishizaka, T. Aizawa, M. Sata, N. Iso-o, E. Noiri, I. Mori, M. Ohno, R. Nagai, Iron chelation and a free radical scavenger suppress angiotensin II-induced upregulation of TGF-beta1 in the heart, Am. J. Physiol. Heart Circ. Physiol. 288 (2005) H1836–H1843.
[35] T. Imamura, M. Takase, A. Nishihara, E. Oeda, J. Hanai, M. Kawabata, K. Miyazono, Smad6 inhibits signalling by the TGF-beta superfamily, Nature 389 (1997) 622–626.

Technical modification of the double-balloon endoscopy to access to the proximal side of the stenosis in the distal colon

Tomonori Yano, MD, Hironori Yamamoto, MD, Hiroto Kita, MD, Keijiro Sunada, MD, Yoshikazu Hayashi, MD, Hiroyuki Sato, MD, Michiko Iwamoto, MD, Yutaka Sekine, MD, Tomohiko Miyata, MD, Akiko Kuno, MD, Makoto Nishimura, MD, Hironari Ajibe, MD, Kenichi Ido, MD, Kentaro Sugano, MD

Tochigi, Japan

Background: The inability to pass endoscopes beyond strictures is a considerable problem in patients with a colonic stricture.

Methods: In patients with bowel obstruction, we have modified the insertion method for double-balloon endoscopy with a long, transnasal decompression tube.

Observations: We have succeeded in reaching the proximal side of the stricture from the oral approach across the entire small bowel in a patient.

Conclusions: This modified double-balloon enteroscopy is useful for patients with bowel obstruction in whom a long decompression tube is already placed.

Double-balloon endoscopy is a novel system that enables endoscopic scrutiny of the entire small bowel.[1-3] We have modified the insertion method of this system for patients with a transnasal, long decompression tube placement for bowel obstruction. We used this modified double-balloon endoscopy in a patient with a narrow segment in the left side of the colon and succeeded in reaching the proximal side of the stricture from an oral approach across the entire small bowel.

PATIENTS AND METHODS

A 45-year-old man was referred to our hospital because of chronic diarrhea and abdominal fullness. A contrast study of the colon revealed a severely strictured lesion from the descending colon to the rectosigmoid colon. The stricture was more likely caused by inflammation than by neoplasm, and a markedly dilated transverse colon also was observed. Before our evaluation, he required emergent hospitalization because of bowel obstruction. A long decompression tube (Ileus tube, soft type, open tip Phycon; Fuji Systems Corp, Tokyo, Japan), (300 cm and diameter of 5.3 mm) was inserted transnasally under fluoroscopic guidance into the jejunum. The tip of the decompression tube has a balloon that was distended by filling with water after insertion of the tube so that the tip could be advanced by peristalsis.

0016-5107/$30.00
PII: S0016-5107(05)00542-0

After the hospitalization, decompression with the long tube relieved his clinical symptoms. An abdominal radiograph taken a few days later showed that the tip of the decompression tube reached the terminal ileum. Colonoscopy, without bowel preparation, demonstrated a stenotic lesion at the rectosigmoid colon, and further endoscopic insertion was not possible. The mucosal surface of the rectum was irregular and suggested diffuse inflammation. Neither ulcers nor erosions were observed in the rectum. A biopsy specimen of the rectal mucosa showed infiltration with inflammatory cells, which suggested chronic inflammation, e.g., ulcerative colitis. A biopsy specimen from the distal edge of the stricture did not reveal any neoplastic changes. To explore the proximal side of the stenosis, we used double-balloon endoscopy (Fujinon EN-450P5/20; Fujinon Corp, Saitama, Japan) (200 cm and diameter of 8.5 mm), with a new modified insertion technique (Fig. 1A to E). The procedure was carried out without any special bowel preparation. Initially, the proximal end of the nasally inserted decompression tube was cut off so that the insertion route could begin from the mouth. The balloon of the decompression tube was inflated with air to fix the tip of the tube in the terminal ileum. A double-balloon-endoscopy overtube was inserted along the decompression tube after stiffening of the tube with a guidewire. The tip of the overtube easily reached the terminal ileum, because the tip of the decompression tube was already at the terminal ileum and was fixed with its balloon. It took 10 minutes for the insertion of the overtube. Then, the overtube balloon was inflated to fix the overtube tip at the terminal ileum. Both the guidewire and the decompression tube were removed, leaving the overtube in place. These procedures

were performed under fluoroscopic guidance with the patient under conscious sedation. Finally, the enteroscope was inserted through the overtube. The enteroscope tip easily reached the terminal ileum within a few minutes. These procedures enabled the insertion of the endoscope to the terminal ileum from an oral approach. The endoscope was further inserted into the colon by way of the ileocecal valve and reached the proximal side of the stricture in the descending colon. No solid stool was packed in the colon, and endoscopic insertion and observation were easily possible by washing some remaining stool on the colonic wall. Irregular mucosa was observed at the proximal edge of the stricture of the descending colon, along with inflammatory changes and ulcerations throughout the entire colon, which suggested pancolitis (Fig. 2). A biopsy

Capsule Summary

What is already known on this topic

- It is sometimes endoscopically impossible to traverse tight colonic strictures.
- Double-balloon endoscopy is a new technique that allows endoscopic visualization of the entire small bowel.

What this study adds to our knowledge

- In a single patient, modified double-balloon enteroscopy was used to traverse the entire small bowel and reach the proximal end of a descending colonic inflammatory stricture.

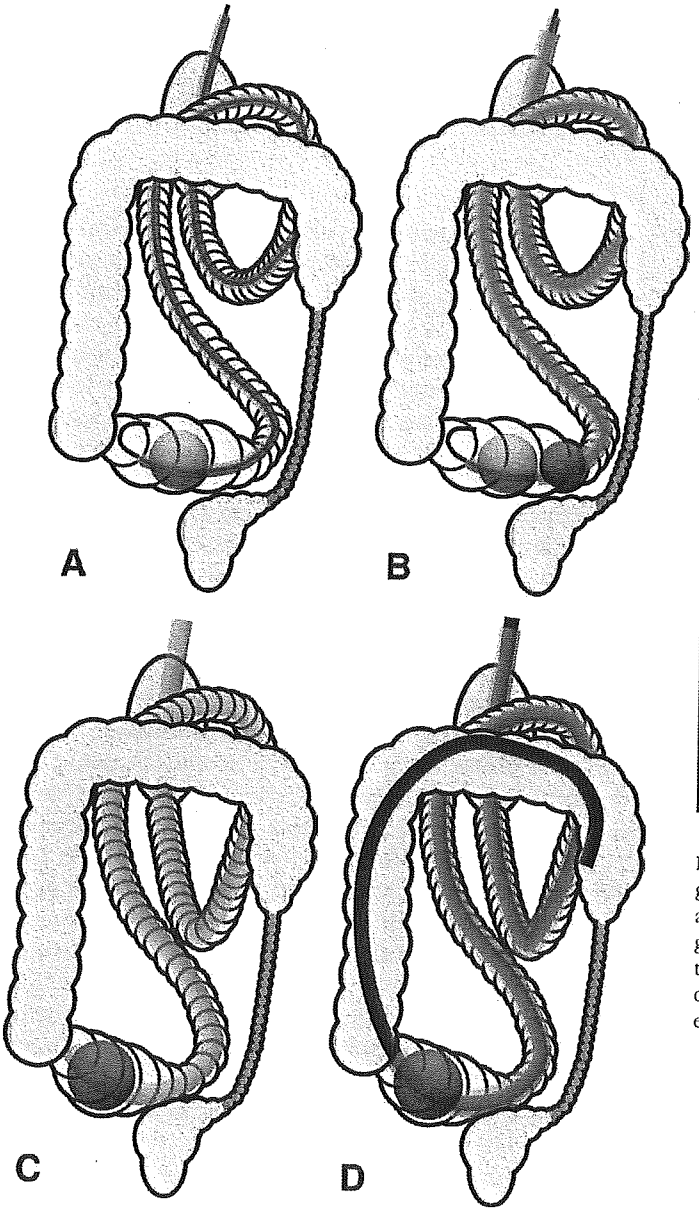

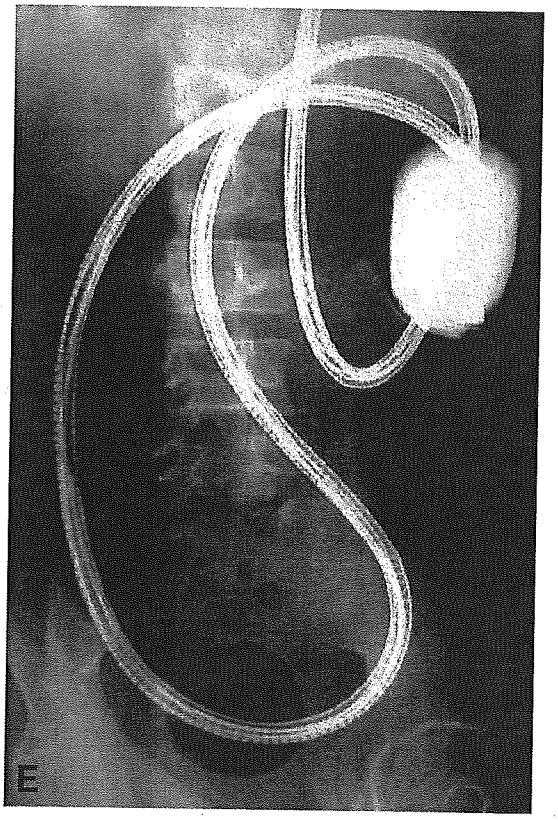

Figure 1. Illustration of the insertion technique. **A,** Insertion of the guidewire through the decompression tube. **B,** Insertion of the overtube along the decompression tube. **C,** Removal of the ileus tube and guidewire after inflation of the balloon at the tip of the overtube to fix the overtube in the intestine **D,** Insertion of enteroscope through the overtube to the stricture in the colon. **E,** Fluoroscopic image of the enteroscope.

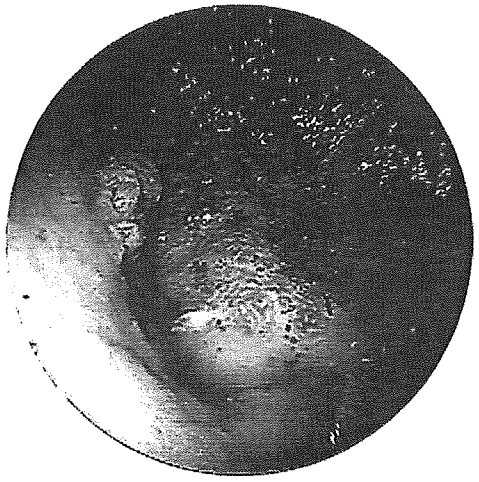

Figure 2. Endoscopic view of the tumor from the proximal side of the stricture.

specimen taken from the irregular mucosa at the edge of the stricture revealed adenocarcinoma. Because the diagnosis of colitic cancer was made before surgery, curative surgery with a total colectomy and a lymph-node resection was performed. Postoperative course was uneventful, and no recurrence was observed during 2 years of follow-up.

DISCUSSION

A major complication of ulcerative colitis and Crohn's disease can be strictures, which should always raise the question of malignancy.[4,5] Ulcerative colitis is one of the risk factors of developing colorectal carcinoma, and screening for cancer is recommended by a number of sources.

Although retrograde colonoscopic techniques have improved, strictures continue to hamper endoscopic access. Capsule endoscopy is a new powerful diagnostic tool, but this new modality cannot be used when strictures are present, because of the risk of entrapment.[6] Although anterograde colonoscopy in a patient with a jejunoileal bypass was previously reported, this is the first report of endoscopic examination of the descending colon from the oral approach in a patient without a surgical bypass or resection of the small intestine.[7] Transnasal, long decompression tube placement is an effective palliative treatment of mechanical bowel obstruction and is commonly used in Japan. The time required for the tip of the decompression tube to reach the distal intestine and to release the obstruction varies from patient to patient and ranges from several hours to several days. The long decompression tube placed into the small intestine was useful for guiding the overtube into the ileum. We previously reported our experience with double-balloon enteroscopy in two cases of oral insertion up to the cecum. In these two cases, the insertion time to the cecum was, on average, 114 minutes.[8] By contrast, it took only a few minutes with this new modified technique for the enteroscope to reach the terminal ileum after overtube placement. This modified double-balloon endoscopy is useful for patients with bowel obstruction in whom a long decompression tube can be placed.

DISCLOSURE

Hironori Yamamoto has applied for the patent in Japan on the double-balloon system described in this article.

REFERENCES

1. Yamamoto H, Sekine Y, Sato Y, Higashizawa T, Miyata T, Iino S, et al. Total enteroscopy with a nonsurgical steerable double-balloon method. Gastrointest Endosc 2001;53:216-20.
2. Yamamoto H, Yano T, Kita H, Sunada K, Ido K, Sugano K. New system of double-balloon enteroscopy for diagnosis and treatment of small intestinal disorders [letter]. Gastroenterology 2003;125:1556, author reply 1557.
3. Yamamoto H, Sugano K. A new method of enteroscopy: the double-balloon method. Can J Gastroenterol 2003;17:273-4.
4. Lashner BA, Turner BC, Bostwick DG, Frank PH, Hanauer SB. Dysplasia and cancer complicating strictures in ulcerative colitis. Dig Dis Sci 1990;35:349-52.
5. Gumaste V, Sachar DB, Greenstein AJ. Benign and malignant colorectal strictures in ulcerative colitis. Gut 1992;33:938-41.
6. Fleischer DE. Capsule endoscopy: the voyage is fantastic: will it change what we do? Gastrointest Endosc 2002;56:452-6.
7. Burton JR Jr, Katon R. Anterograde colonoscopy: per oral diagnosis of colon cancer with an enteroscope in a man with a jejunoileal bypass. Gastrointest Endosc 2003;57:982-3.
8. Yamamoto H, Kita H, Sunada K, Hayashi Y, Sato H, Yano T, et al. Clinical outcomes of double-balloon endoscopy for the diagnosis and treatment of small-intestinal diseases. Clin Gastroenterol Hepatol 2004;10:1010-6.

Received October 20, 2004. Accepted March 7, 2005.

Current affiliations: Department of Internal Medicine, Division of Gastroenterology, Jichi Medical School, Tochigi, Japan.

Meeting presentations: American Society for Gastrointestinal Endoscopy poster session, Digestive Disease Week May 15-20, 2004, New Orleans, Louisiana (Gastrointest Endosc 2004;59:AB269).

Reprint requests: Hironori Yamamoto, MD, Department of Internal Medicine, Division of Gastroenterology, Jichi Medical School, Yakushiji, Minamikawachi, Tochigi, 329-0498, Japan.

日消誌　2005；102：866—872

今月のテーマ●胆管癌の診断と治療

内科の立場から

玉　田　喜　一　　菅　野　健太郎[1)]

要旨：胆管癌の早期診断には胆管拡張例に magnetic resonance cholangiopancreatography を施行し，内視鏡的逆行性膵胆道造影時に intraductal ultrasonography と胆管生検を行う．進展度診断には multidetector row-CT と intraductal ultrasonography が有用である．胆管癌の治療には多くのオプションがあり，入院早期から内科医と外科医が十分に連絡をとり，診断を進める事が大切である．保存的治療では，メタリックステントが有用である．ステント内への腫瘍増殖を防ぐために腫瘍の局所制御を十分行う必要がある．ステント閉塞時の対処も大切である．

索引用語：胆管癌，ERCP，IDUS，ステント

はじめに

胆管癌はその占拠部位および肉眼形により多彩な臨床経過を辿る．胆道ドレナージ法の選択も手術適応に対する考え方も，施設ごとに異なる．また，欧米では本邦と異なり，超音波検査（Ultrasonography；US）で閉塞性黄疸と診断された症例に magnetic resonance cholangiopancreatography（MRCP）による質的診断を行い，更に multidetector-row CT（MDCT）による進展度診断を行い，胆道ドレナージを施行せずに根治術を施行する事が，治療費軽減および入院期間短縮に有用であると主張されている．本稿では，日本の医療状況で有用な話を述べる．特に，胆管癌の診断と治療における内科医の役割を述べる．

I　胆管癌のスクリーニング

家庭医を含めた内科医は腹部不快感を訴える患者，検診で肝障害，胆道系酵素上昇を指摘された患者の中から胆管癌患者を拾い上げる事が大切な仕事である．本邦では超音波診断装置が家庭医にも普及しており，腹部不快感を訴える患者がUSを受ける機会は増加している．また，成人病検診，職場健診等で血液生化学検査を受ける機会も多いため，無黄疸の胆管癌を発見するきっかけは欧米より多いと考える[1)2)]．

II　無黄疸胆管癌の診断（Figure 1）

1．US

無黄疸の胆管癌患者がUSを受けた時，上部胆管に位置する腫瘍は描出率が高いが，膵内胆管は十二指腸ガスの影響で十分な描出は困難である．深い左側臥位として観察すると消化管ガスが移動し肝外胆管の描出はある程度向上する．総胆管径が7mm以上であった患者に超音波内視鏡を prospective に施行した報告では，14％で胆管癌を含む胆道癌が発見されている[3)]．したがって胆管拡張例では下部胆管の腫瘍を考慮し，更なる精査を施行すべきである．

2．MRCP

これまでは造影剤を用いずに下部胆管の腫瘍を評価する手法として超音波内視鏡が活用されてきた[3)]．現在ではMRIを応用したMRCPが普及した．MRIのT2強調画像では造影剤を用いなくても，動きの遅い液体が高シグナルとなるため，胆管と膵管が描出される．CTと異なりレントゲン被曝もなく患者の苦痛もないため，USの次に位

1）自治医科大学内科学消化器内科部門

Diagnosis and treatment of bile duct cancer—from the viewpoint of physician—

Kiichi TAMADA and Kentaro SUGANO[1)]

1）Division of Gastroenterology, Jichi medical school

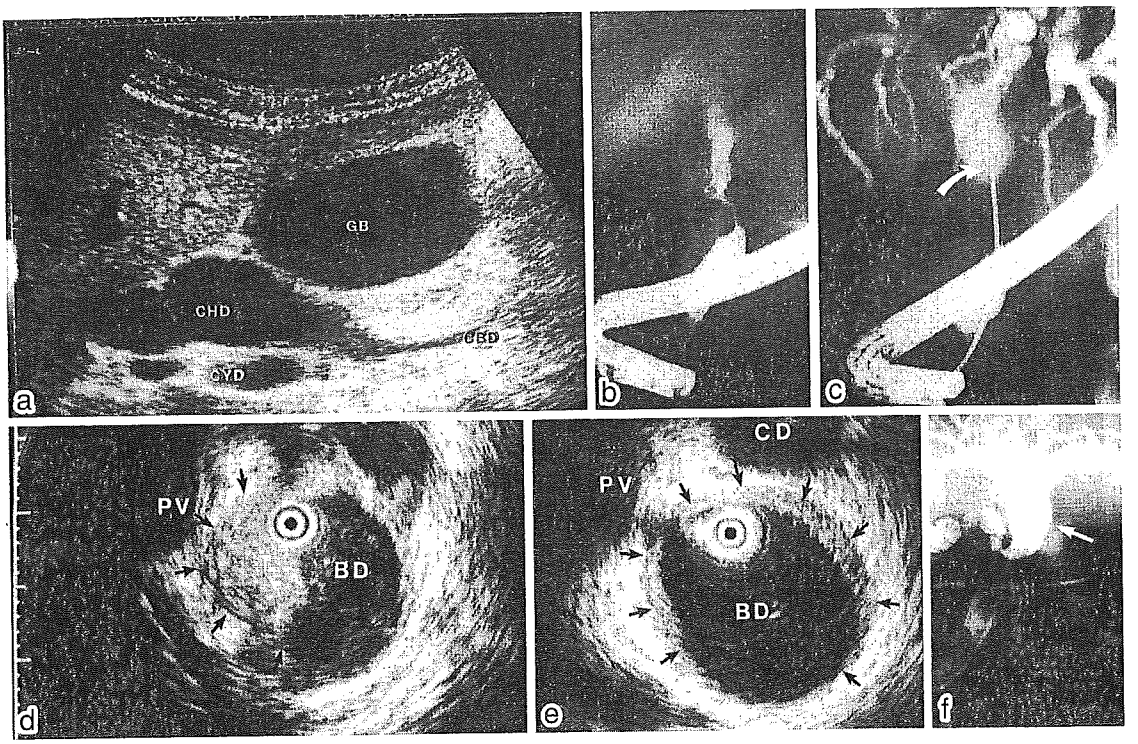

Figure 1. 無黄疸胆管癌の診断：Diagnosis of unicteric bile duct carcinoma **a**：超音波所見；黄疸は認めなかったが検診目的の超音波で総肝管（CHD）と胆嚢（GB）の拡張，中部胆管の壁肥厚を認めた．**b**：胆道造影；中部胆管に狭窄を認める．**c**：胆道造影；Intraductal ultrasonography（IDUS）のプローブが挿入されている（矢印）．**d**：IDUS 画像；中部胆管（BD）で壁構造中断をともなう腫瘍（矢印：T）を認めた．門脈（PV）浸潤を認めない．**e**：IDUS 画像；上部胆管（BD）で偏周性の壁肥厚（矢印）を認め，腫瘍の進展と判断した．この所見は左右肝管分岐部まで認められた．胆嚢管（CD）が描出されている．**f**：経鼻胆道ドレナージからの胆道造影；造影では上部胆管（矢印）まで胆管壁硬化所見を認めたが，病理所見では左右肝管分岐部までの腫瘍進展が確認された．

置づけられる二次スクリーニング法である．無黄疸胆管癌の診断に有用である[4]．MRCP で胆管狭窄が疑われれば次に述べる内視鏡的逆行性膵胆道造影（Endoscopic retrograde cholangiopancreatography；ERCP）に進む．

3. ERCP

熟練者が施行してもまれに膵炎を生じるため，検査入院が必要．乳頭部を直接観察し生検できるため，Vater 乳頭部癌の診断に極めて有用である．現在 MRCP の解像力は向上しており，単に造影を行うだけの ERCP では，MRCP を超える情報が得られない事がある．したがって MRCP で胆管狭窄が疑われた症例に対しては胆管生検と胆管内超音波検査法（intraductal ultrasonography；IDUS）の準備をして ERCP を施行する事が胆管癌の早期診断につながる[1)2)5)]．

4. IDUS

根本的に，US 診断装置は高周波であるほど距離分解能は向上するが，エコー減衰のため，有効描出深度は浅くなる．通常の体外 US の使用周波数は 3～4MHz である．周波数 20MHz の高周波プローブは，距離分解能は 0.1mm と優れているが，有効描出深度は 2cm 以下である．したがって高周波プローブを腹壁の上からあてても腹腔内臓器の描出はできない．

IDUS に用いる高周波プローブは 2mm と細径で内視鏡鉗子孔から挿入可能で，先端にガイドワイヤ誘導スリットが付いているため乳頭括約筋切開術を施行せずに ERCP 時に胆管内に挿入可能である．胆管内から走査する事で消化管ガスの影響を受けずに胆管の詳細な画像が得られる．IDUS は微細な病変描出に優れているが，描出された病

変がすべて悪性なわけではなく，胆管壁構造，腫瘍径，茎の形状による良悪性の検討が必要である[2)5)]．早期癌が少ないため欧米の診断基準は，わが国では有用でない．

5．経乳頭的胆管生検

ERCP施行時に胆管内にガイドワイヤを留置し，その上縁を沿わせる形で生検鉗子を胆管内に挿入する[2)5)6)]．内視鏡直視下でなく透視下の生検となる．欧米で多用されている生検システムでは胆管癌の生検陽性率は30～40%と低率である．わが国では径1.8mmのテフロンコーティングの生検鉗子が多用され，胆管癌での生検陽性率は80%以上である[2)5)6)]．

6．経口親子式胆道鏡

膵管鏡として開発された高解像度の電子スコープは胆道鏡としても使用可能である．3.4mm径と従来の胆道鏡より細径でありながら，鮮明な画像が得られる．ステント挿入等に使用する処置用スコープ（親スコープ）の鉗子孔から細径胆道鏡（子スコープ）が挿入できる[7)]．経口胆道鏡下の直視下生検は理論的には優れているはずだが，現時点では透視下の胆管生検の成績に及ばない．子スコープの鉗子孔から挿入可能な生検鉗子が細く，採取できる組織が透視下生検より小さい．

III 閉塞性黄疸に対する胆道ドレナージ

1．中下部胆管癌

閉塞性黄疸例，胆管炎をともなう例では胆道ドレナージが必要となる．胆管炎をともなわない中下部胆管癌ではドレナージなしで根治術が行われる事もある．かつては術前減黄は経皮経肝的胆道ドレナージ（Percutaneous transhepatic biliary drainage；PTBD）が主流であったが，内視鏡的経鼻胆道ドレナージ（Endoscopic naso-biliary drainage；NBD）の技術，機器が進歩し，安全なドレナージ法として術前減黄としても活用されている．特に中下部胆管閉塞ではERCPに引き続きNBDを施行する事で，乳頭部の観察と膵管造影を施行し，乳頭部癌，膵癌との鑑別がドレナージと同時に行える．

2．肝門部胆管癌

肝門部胆管狭窄のドレナージ法の選択にはまずMRCPを施行し左右肝管および肝内胆管の分断状態を把握したい．NBDは現実的に1本しか挿入できないので，左右肝管分断例の術前全肝ドレナージにはPTBDの複数本挿入が必要となる．経乳頭的にプラスチックステントを複数本挿入する事は容易だが，胆管癌に内視鏡的胆管ステントを挿入しては術前検査が困難となる[8)]．胆管像も得る事ができず，切除線の決定もできない．特に肝門部胆管癌術前に内視鏡的胆管ステントを挿入し，下端が十二指腸に出た状態で紹介されるのは最悪である．分断された肝内胆管に胆管炎を生じると悲惨な状態になる．NBDのままで専門施設に紹介した方がよい．NBDなら転院後に新たに胆管像を得る事も可能である．術前精査の胆道鏡，あるいは胆道鏡下局所治療のためにPTBDルートが必要な時は，NBDをクランプし映像下にPTBDが可能である[9)10)]．

肝門部分断例でも，はじめから全肝ドレナージを目指さずに術後に残す予定の肝側にNBDを挿入する方法もある．片方の肝管，たとえば左肝管原発の腫瘍があっても，右肝管が開存している間は黄疸は呈さない．右肝管まで閉塞が及んだ時に黄疸が出現する．NBDではこの場合，残す予定の右肝管側の方が狭窄も軽度でガイドワイヤも進みやすい．直前まで機能していた肝側のため，反対側の胆管炎を生じなければ，1本のNBDで減黄可能である．これに対して，PTBDを選択した場合，最もエコー下穿刺が容易な拡張胆管を穿刺したくなるが，左右分断例では胆管拡張が高度な側は切除予定側の肝臓であり，長期に機能していない肝臓のため，減黄には反対側の肝臓の追加ドレナージが必要となる．

IV 胆管癌の進展度診断

1．Multidetector-row CT（MDCT）

MDCTの登場で飛躍的に高速な撮像が可能となり，微細な病変の評価が可能となった．また，従来の横断像のみでなくmultiplanar reformation（MPR），curved planar reformation（CPR）等の再構成画像による多方向からの観察が可能となった．特に総胆管を一断面に描出するCPRの画像は胆管癌と周囲臓器の関係がわかりやすく美し

い[11]．

肝門部胆管癌の右肝動脈浸潤の正診率94%，門脈浸潤の正診率91%と，優れた成績が報告されている[12]．従来のカテーテルを用いた診断目的の血管造影は不要となり，われわれの施設でも施行していない．

2．Fluorodeoxyglucose positron emission tomography（FDG-PET）

PETは陽電子放出核種を用い，生体内の生理生科学的機能を画像化する．FDGを用い，糖代謝が亢進している腫瘍細胞への取り込みを見る．最近の報告では結節型胆管癌の陽性率は良好だが浸潤型胆管癌の陽性率は不良である．活動性胆管炎をともなう原発性硬化性胆管炎，留置した胆管ステント周囲等にFDGの集積が報告されているため注意が必要である．胆道癌はPETの保険適応になっていない．現時点では胆管癌の存在診断にPETが使用される事はないが，リンパ節転移を含めた遠隔転移の診断には有用であり，保険適応となれば，不必要な手術を減らす事には貢献できる[13]．

3．IDUS

現時点ではIDUSの距離分解能はMDCTより優れており，門脈浸潤，肝動脈浸潤，膵浸潤等の診断に活用されている[14][15]．ただし，エコー減衰のため，肝十二指腸間膜外の情報はMDCTが必要である．

V　水平方向の進展

1．経皮経肝的胆道鏡（Percutaneous transhepatic cholangioscopy；PTCS）

胆管癌は胆管像で描出される範囲を超えて胆管長軸方向の粘膜下進展または粘膜表層進展を呈する事が知られている[10][14][15]．PTCSによるmapping biopsyが胆管癌切除線決定のために行われてきた[10]．われわれも胆管拡張をともなわない無黄疸症例にPTCSを施行する手法も確立し，術前に切除線を決定してきた[9][10]．しかし，PTBDルートへの癌播種が問題視[16]されてからは施行していない．

2．IDUS

IDUSが登場した時に最も期待されたのが胆管水平方向進展の診断である．しかし，胆管壁の肥厚は癌の進展のみでなく，ドレナージカテーテルによる機械的刺激でも認められた[17]．ドレナージ施行前の初回ERCP時にIDUSを施行する事でアーチファクトが最小限となり診断率が向上する[18]．

3．Virtual cholangioscopy

MRCPおよびCTの3D画像を利用したvirtual cholangioscopyも臨床活用されているが，顆粒状粘膜および腫瘍血管の描出はできないので，胆管癌の水平方向進展診断には有用ではない．

4．MDCT

浸潤型胆管癌ではMDCTで粘膜下浸潤部が濃染する壁肥厚像として描出される事があり，肝門部胆管癌の進展範囲の進展に利用される[12][19]．ドレナージ施行後に胆管壁肥厚が生じてしまうため，IDUS同様にドレナージ前にMDCTを施行する事が望ましい．もちろん，粘膜内進展の描出は困難である．

VI　治療法の選択

以上述べたごとく画像診断は進歩した．しかし今日でも，手術すべきか保存的治療を選ぶべきか迷う症例は多い．入院早期から内科医と外科医が十分に連絡をとり，診断を進める事が大切である．もちろん，患者の人生観が大切である．手術を受ける意志がないなら，術前検査を省略し集学的治療を早めに進めるべきである．

VII　胆道内瘻術

1．Plastic stent

保存的治療が選択された場合，最も患者の生活の質に直結するのが閉塞性黄疸の管理であり，胆管ステント療法が行われる．径7～12Fr，フラップ間の長さが5～12cmのプラスチックステントが各社から市販されており，ERCP用内視鏡の鉗子孔を通して胆管内に挿入できる．1本1～2万円と，後述するmatallic stentの1/10以下の価格である．閉塞時に内視鏡的に抜去し交換できる．胆泥による閉塞のため数カ月ごとの入れ替えが必要となる．

2．Metallic stent

Metallic stentはメッシュ構造となっており，

2.3～3mmの細径のイントロデューサーを用いてERCP用内視鏡の鉗子孔を通して胆管内に挿入した後に，自己拡張力で8～10mm径に広がる．PTBDルートからも同様の細さで挿入可能である．Uncovered metallic stentはメッシュ構造がむき出しになっており，肝内胆管で側枝を塞がないのが利点である．放射線療法等で腫瘍の局所制御がされている症例では長期の開存が期待できるが，局所が十分制御されない症例では腫瘍がメッシュ間に増殖して閉塞する(tumor ingrowth)[20]．メッシュで胆管壁に密着するため逸脱しないが，一端挿入すると抜去には大変な労力を要する[21]．したがって良性胆管狭窄を悪性と誤診してmetallic stentを挿入すると，数年以内にstentが豆腐の中に網がめり込むように胆管壁に埋没してしまい，異物化し結石が形成され悲惨な状態となる．

肝門部閉塞に対しては従来，左右からPTBDを施行し，複数本のmatallic stent挿入が行われてきた．しかし最近の報告では切除不能の肝門部閉塞に対しては片側への内視鏡的なmetallic stent挿入でよいとされている[22]．先に述べたように，PTBD例ではまず拡張の高度な肝内胆管にドレナージが行われる傾向があるが，ERCPでは狭窄が軽度な方，つまり機能が保たれている肝側の胆管にガイドワイヤが進みやすい．

3. Covered metallic stent

Covered metallic stentはUncovered metallic stentの欠点であるtumor ingrowthを防ぐために開発され数社から市販されている．分岐を閉塞してしまうので肝門部胆管には使用できないが，中下部胆管閉塞では極めて有効である[23]．内視鏡的な抜去が可能[21]だが逸脱も生じる．

VIII 局所療法

1. 放射線療法

胆管癌の局所療法はmetallic stent内へのtumor ingrowthを押さえる意味でも有用である．かつては胆管癌への体外照射は無効とされていたが，55Gr以上の高線量照射で生存期間の延長が報告されている[24]．高線量照射による消化管出血が問題となるが，内視鏡治療で対処できる[25]．腔内照射も有用であり，ステントが不要になれば理想的である[26]．

2. Photodynamic theraphy (PDT)

腫瘍親和性光感受性物質とレーザー光照射による光化学反応を応用した光線力学的治療法(photodynamic theraphy；PDT)の報告も見られる．光線過敏症対策に4週間の遮光が必要である．経乳頭的に施行し，無効で高率(50%)に胆管炎を生じたという報告[27]と有用であったという報告[28]が見られる．PTCS下に安全に施行し有用であったという報告も見られる[29]．胆管癌に対するPDTは保険適応外であり，施行できる施設は限られる．

3. マイクロ波焼却法

マイクロ波加熱は電界内における誘導体の分極現象を高い周波数で交互に繰り返しおこす事により電解エネルギーを誘導体に吸収させ発熱させる加熱法である．内視鏡的止血術や肝臓癌の治療に多用されている．PTCS下に腫瘍焼却療法を行い胆管の開通が得る事ができる[30]．

IX 化学療法

膵癌に対して有効なGemcitabineは，欧米では胆管癌に対しても投与され，単剤投与[31]および多剤併用療法で有効性と安全性が確認されている．本邦でも現実的には胆管癌への投与が行われ症例が蓄積されつつある．吐き気等の副作用が少なく，使用しやすい薬剤である．現在では自費診療となってしまうため，早く保険適応となる事が待たれる．

X 保存療法選択後 (Figure 2)

保存的療法を選択した場合，ステント挿入後の長期的な管理は，内科医にとって大切な課題である．胆管ステントが再閉塞した場合に，患者は夜間休日等に胆管炎を生じて来院するため，当直を行う若手医師等の教育も肝要である．胆管ステント閉塞時の胆管炎は，腹痛は生じない．発熱のみが前景にでる．したがって，安易に感冒等と判断して帰宅させる事がないように，ステント挿入時の患者が発熱で来院した時は，採血にて胆道系酵素の上昇等をきちんと調べるように，外来カルテ等に記載しておく事が大切である．

metallic stent挿入後は，MRCPではステント部位が消しゴムで消したような画像となり情報は得